USGS
science for a changing world

Germanium and Indium

Chapter I of

Critical Mineral Resources of the United States—Economic and Environmental Geology and Prospects for Future Supply

Professional Paper 1802–I

U.S. Department of the Interior
U.S. Geological Survey

Periodic Table of Elements

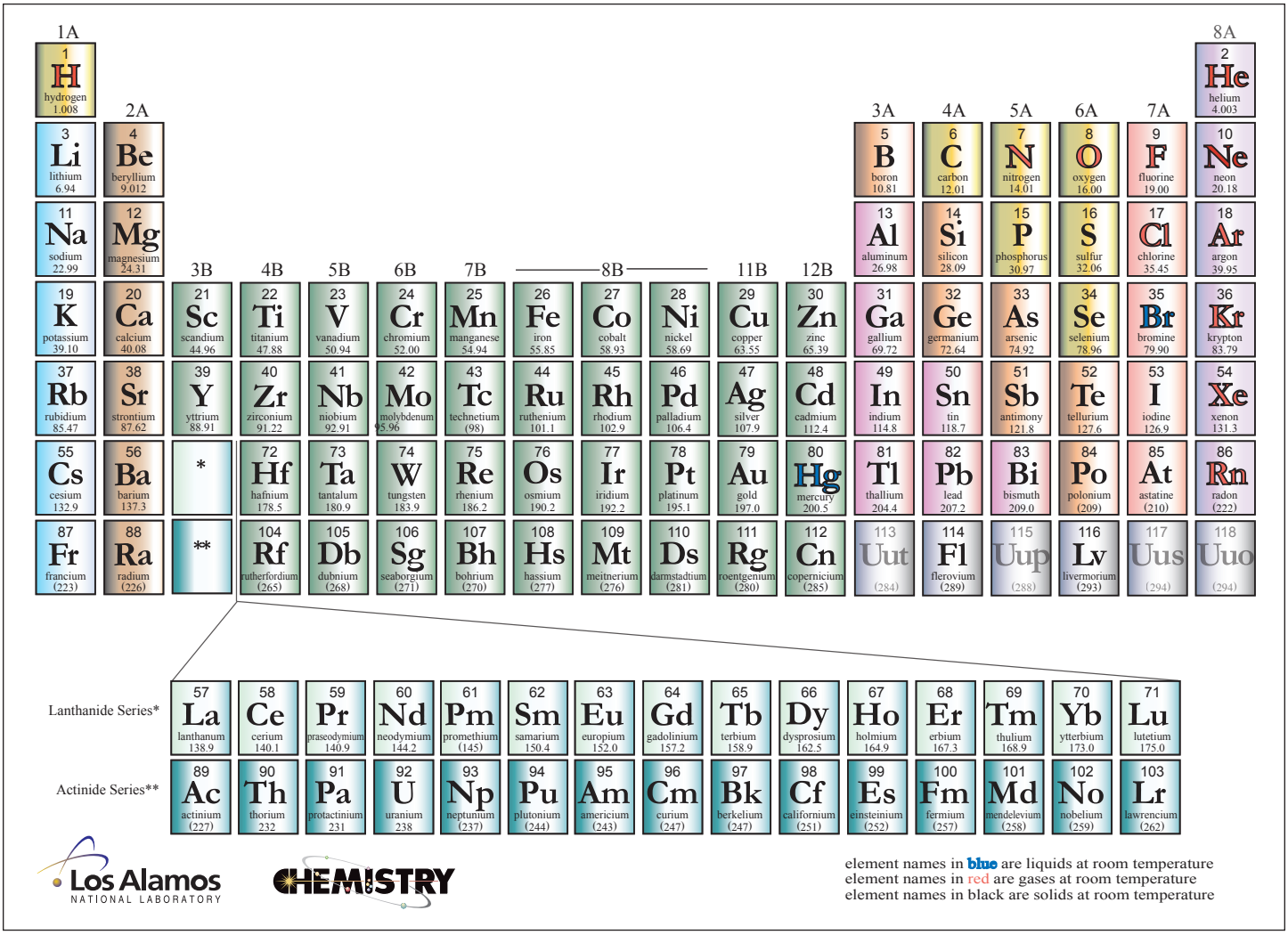

Modified from Los Alamos National Laboratory Chemistry Division; available at http://periodic.lanl.gov/images/periodictable.pdf.

Cover. Left, concentrator photovoltaic solar power system that uses germanium-based solar power cells. Photograph courtesy of Arzon Solar, LLC. Right, flat-panel display screens and touchscreens coated with indium oxide. Photograph courtesy of CI Systems, Inc.

Germanium and Indium

By W.C. Pat Shanks III, Bryn E. Kimball, Amy C. Tolcin, and David E. Guberman

Chapter I of

Critical Mineral Resources of the United States—Economic and Environmental Geology and Prospects for Future Supply

Edited by Klaus J. Schulz, John H. DeYoung, Jr., Robert R. Seal II, and Dwight C. Bradley

Professional Paper 1802–I

U.S. Department of the Interior
U.S. Geological Survey

U.S. Department of the Interior
RYAN K. ZINKE, Secretary

U.S. Geological Survey
William H. Werkheiser, Acting Director

U.S. Geological Survey, Reston, Virginia: 2017

Suggested citation:
Shanks, W.C.P., III, Kimball, B.E., Tolcin, A.C., and Guberman, D.E., 2017, Germanium and indium, chap. I *of* Schulz, K.J., DeYoung, J.H., Jr., Seal, R.R., II, and Bradley, D.C., eds., Critical mineral resources of the United States—Economic and environmental geology and prospects for future supply: U.S. Geological Survey Professional Paper 1802, p. I1–I27, https://doi.org/10.3133/pp1802I.

ISSN 2330-7102 (online)

Contents

Figures

Tables

Conversion Factors

International System of Units to Inch/Pound

Multiply	By	To obtain
	Length	
angstrom (Å) (0.1 nanometer)	0.003937	microinch
angstrom (Å) (0.1 nanometer)	0.000003937	mil
micrometer (µm) [or micron]	0.03937	mil
millimeter (mm)	0.03937	inch (in.)
centimeter (cm)	0.3937	inch (in.)
meter (m)	3.281	foot (ft)
meter (m)	1.094	yard (yd)
kilometer (km)	0.6214	mile (mi)
	Area	
hectare (ha)	2.471	acre
square kilometer (km^2)	247.1	acre
square meter (m^2)	10.76	square foot (ft^2)
square centimeter (cm^2)	0.1550	square inch (ft^2)
square kilometer (km^2)	0.3861	square mile (mi^2)
	Volume	
milliliter (mL)	0.03381	ounce, fluid (fl. oz)
liter (L)	33.81402	ounce, fluid (fl. oz)
liter (L)	1.057	quart (qt)
liter (L)	0.2642	gallon (gal)
cubic meter (m^3)	264.2	gallon (gal)
cubic centimeter (cm^3)	0.06102	cubic inch (in^3)
cubic meter (m^3)	1.308	cubic yard (yd^3)
cubic kilometer (km^3)	0.2399	cubic mile (mi^3)
	Mass	
microgram (µg)	0.00000003527	ounce, avoirdupois (oz)
milligram (mg)	0.00003527	ounce, avoirdupois (oz)
gram (g)	0.03527	ounce, avoirdupois (oz)
gram (g)	0.03215075	ounce, troy
kilogram (kg)	32.15075	ounce, troy
kilogram (kg)	2.205	pound avoirdupois (lb)
ton, metric (t)	1.102	ton, short [2,000 lb]
ton, metric (t)	0.9842	ton, long [2,240 lb]
	Deposit grade	
gram per metric ton (g/t)	0.0291667	ounce per short ton (2,000 lb) (oz/T)
	Pressure	
megapascal (MPa)	10	bar
gigapascal (GPa)	10,000	bar
	Density	
gram per cubic centimeter (g/cm^3)	62.4220	pound per cubic foot (lb/ft^3)
milligram per cubic meter (mg/m^3)	0.00000006243	pound per cubic foot (lb/ft^3)
	Energy	
joule (J)	0.0000002	kilowatthour (kWh)
joule (J)	6.241×10^{18}	electronvolt (eV)
joule (J)	0.2388	calorie (cal)
kilojoule (kJ)	0.0002388	kilocalorie (kcal)

International System of Units to Inch/Pound

Multiply	By	To obtain
	Radioactivity	
becquerel (Bq)	0.00002703	microcurie (μCi)
kilobecquerel (kBq)	0.02703	microcurie (μCi)
	Electrical resistivity	
ohm meter (Ω-m)	39.37	ohm inch (Ω-in.)
ohm-centimeter (Ω-cm)	0.3937	ohm inch (Ω-in.)
	Thermal conductivity	
watt per centimeter per degree Celsius (watt/cm °C)	693.1798	International British thermal unit inch per hour per square foot per degree Fahrenheit (Btu in/h ft^2 °F)
watt per meter kelvin (W/m-K)	6.9318	International British thermal unit inch per hour per square foot per degree Fahrenheit (Btu in/h ft^2 °F)

Inch/Pound to International System of Units

	Length	
mil	25.4	micrometer (μm) [or micron]
inch (in.)	2.54	centimeter (cm)
inch (in.)	25.4	millimeter (mm)
foot (ft)	0.3048	meter (m)
mile (mi)	1.609	kilometer (km)
	Volume	
ounce, fluid (fl. oz)	29.57	milliliter (mL)
ounce, fluid (fl. oz)	0.02957	liter (L)
	Mass	
ounce, avoirdupois (oz)	28,350,000	microgram
ounce, avoirdupois (oz)	28,350	milligram
ounce, avoirdupois (oz)	28.35	gram (g)
ounce, troy	31.10 348	gram (g)
ounce, troy	0.03110348	kilogram (kg)
pound, avoirdupois (lb)	0.4536	kilogram (kg)
ton, short (2,000 lb)	0.9072	ton, metric (t)
ton, long (2,240 lb)	1.016	ton, metric (t)
	Deposit grade	
ounce per short ton (2,000 lb) (oz/T)	34.285714	gram per metric ton (g/t)
	Energy	
kilowatthour (kWh)	3,600,000	joule (J)
electronvolt (eV)	1.602×10^{-19}	joule (J)
	Radioactivity	
microcurie (μCi)	37,000	becquerel (Bq)
microcurie (μCi)	37	kilobecquerel (kBq)

Temperature in degrees Celsius (°C) may be converted to degrees Fahrenheit (°F) as follows:

$$°F = (1.8 \times °C) + 32$$

Temperature in degrees Celsius (°C) may be converted to kelvin (K) as follows:

$$K = °C + 273.15$$

Temperature in degrees Fahrenheit (°F) may be converted to degrees Celsius (°C) as follows:

$$°C = (°F - 32) / 1.8$$

Datum

Unless otherwise stated, vertical and horizontal coordinate information is referenced to the World Geodetic System of 1984 (WGS 84). Altitude, as used in this report, refers to distance above the vertical datum.

Supplemental Information

Specific conductance is given in microsiemens per centimeter at 25 degrees Celsius (µS/cm at 25 °C).

Concentrations of chemical constituents in soils and (or) sediment are given in milligrams per kilogram (mg/kg), parts per million (ppm), or parts per billion (ppb).

Concentrations of chemical constituents in water are given in milligrams per liter (mg/L), micrograms per liter (µg/L), nanogams per liter (ng/L), nanomoles per kilogram (nmol/kg), parts per million (ppm), parts per billion (ppb), or parts per trillion (ppt).

Concentrations of suspended particulates in water are given in micrograms per gram (µg/g), milligrams per kilogram (mg/kg), or femtograms per gram (fg/g).

Concentrations of chemicals in air are given in units of the mass of the chemical (milligrams, micrograms, nanograms, or picograms) per volume of air (cubic meter).

Activities for radioactive constituents in air are given in microcuries per milliliter (µCi/mL).

Deposit grades are commonly given in percent, grams per metric ton (g/t)—which is equivalent to parts per million (ppm)—or troy ounces per short ton (oz/T).

Geologic ages are expressed in mega-annum (Ma, million years before present, or 10^6 years ago) or giga-annum (Ga, billion years before present, or 10^9 years ago).

For ranges of years, "to" and (or) the en dash ("–") mean "up to and including."

Concentration unit	Equals
milligram per kilogram (mg/kg)	part per million
microgram per gram (µg/g)	part per million
microgram per kilogram (µg/kg)	part per billion (10^9)

Equivalencies

part per million (ppm): 1 ppm = 1,000 ppb = 1,000,000 ppt = 0.0001 percent
part per billion (ppb): 0.001 ppm = 1 ppb = 1,000 ppt = 0.0000001 percent
part per trillion (ppt): 0.000001 ppm = 0.001 ppb = 1 ppt = 0.0000000001 percent

Metric system prefixes

tera- (T-)	10^{12}	1 trillion
giga- (G-)	10^9	1 billion
mega- (M-)	10^6	1 million
kilo- (k-)	10^3	1 thousand
hecto- (h-)	10^2	1 hundred
deka- (da-)	10	1 ten
deci- (d-)	10^{-1}	1 tenth
centi- (c-)	10^{-2}	1 hundredth
milli- (m-)	10^{-3}	1 thousandth
micro- (µ-)	10^{-6}	1 millionth
nano- (n-)	10^{-9}	1 billionth
pico- (p-)	10^{-12}	1 trillionth
femto- (f-)	10^{-15}	1 quadrillionth
atto- (a-)	10^{-18}	1 quintillionth

Abbreviations and Symbols

°C	degree Celsius
AMD	acid mine drainage
CIGS	copper-indium-gallium-diselenide
CPV	concentrator photovoltaic
CRD	carbonate replacement deposit
EC_{50}	effective concentration 50 (concentration that results in 50 percent exhibiting decreased functionality)
ICP–MS	inductively coupled plasma-mass spectrometry
ITO	indium-tin oxide
LC_{50}	lethal concentration 50 (concentration that kills 50 percent of test population within a given timeframe)
LED	light-emitting diode
m	meter
Ma	mega-annum
mg/L	milligram per liter
MVT	Mississippi Valley-type
NREL	National Renewable Energy Laboratory
OSHA	Occupational Safety and Health Administration
PET	polyethylene terephthalate
PGE	platinum-group element
pg/m^3	picogram per cubic meter
ppb	part per billion
ppm	part per million
ppt	part per trillion
SEDEX	sedimentary exhalative
USGS	U.S. Geological Survey
VMS	volcanogenic massive sulfide

Germanium and Indium

By W.C. Pat Shanks III, Bryn E. Kimball, Amy C. Tolcin, and David E. Guberman

Abstract

Germanium and indium are two important elements used in electronics devices, flat-panel display screens, light-emitting diodes, night vision devices, optical fiber, optical lens systems, and solar power arrays. Germanium and indium are treated together in this chapter because they have similar technological uses and because both are recovered as byproducts, mainly from copper and zinc sulfides.

The world's total production of germanium in 2011 was estimated to be 118 metric tons. This total comprised germanium recovered from zinc concentrates, from fly ash residues from coal burning, and from recycled material. Worldwide, primary germanium was recovered in Canada from zinc concentrates shipped from the United States; in China from zinc residues and coal from multiple sources in China and elsewhere; in Finland from zinc concentrates from the Democratic Republic of the Congo; and in Russia from coal.

World production of indium metal was estimated to be about 723 metric tons in 2011; more than one-half of the total was produced in China. Other leading producers included Belgium, Canada, Japan, and the Republic of Korea. These five countries accounted for nearly 95 percent of primary indium production.

Deposit types that contain significant amounts of germanium include volcanogenic massive sulfide (VMS) deposits, sedimentary exhalative (SEDEX) deposits, Mississippi Valley-type (MVT) lead-zinc deposits (including Irish-type zinc-lead deposits), Kipushi-type zinc-lead-copper replacement bodies in carbonate rocks, and coal deposits.

More than one-half of the byproduct indium in the world is produced in southern China from VMS and SEDEX deposits, and much of the remainder is produced from zinc concentrates from MVT deposits. The Laochang deposit in Yunnan Province, China, and the VMS deposits of the Murchison greenstone belt in Limpopo Province, South Africa, provide excellent examples of indium-enriched deposits. The SEDEX deposits at Bainiuchang, China (located in southeastern Yunnan Province), and the Dabaoshan SEDEX deposit (located in the Nanling region of China) contain indium-enriched sphalerite. Another major potential source of indium occurs in the polymetallic tin-tungsten belt in the Eastern Cordillera of the Andes Mountains of Bolivia. Deposits there occur as dense arrays of narrow, elongate, indium-enriched tin oxide-polymetallic sulfide veins in volcanic rocks and porphyry stocks.

Information about the behavior of germanium and indium in the environment is limited. In surface weathering environments, germanium and indium may dissolve from host minerals and form complexes with chloride, fluoride, hydroxide, organic matter, phosphate, or sulfate compounds. The tendency for germanium and indium to be dissolved and transported largely depends upon the pH and temperature of the weathering solutions. Because both elements are commonly concentrated in sulfide minerals, they can be expected to be relatively mobile in acid mine drainage where oxidative dissolution of sulfide minerals releases metals and sulfuric acid, resulting in acidic pH values that allow higher concentrations of metals to be dissolved into solution.

Introduction

Background

This chapter provides an update of the U.S. Geological Survey (USGS) assessment of germanium and indium resources published in the early 1970s (Weeks, 1973); developments in shorter-term resource availability are addressed in the periodical USGS minerals information reports (part of the U.S. Bureau of Mines from 1925 through 1995). Germanium and indium are in significant demand for high-technology applications, and this has led to many studies of concentrations and distributions in primary mineral deposits, advances in extraction technology for these byproduct elements, increased attention on recycling, a flourishing field developing new applications for these elements and their compounds, and consideration of the impacts that increased consumption could have on the environment.

Germanium

In 1864, English chemist John Newlands postulated the existence of an element that would be intermediate between silicon and tin in his scheme of elemental octaves (Newlands, 1864). In 1871, the salient properties of the undiscovered element were predicted by the Russian chemist Dmitri Mendeleev (Weeks, 1932), who called it ekasilicon (beyond silicon). In 1886, the element was isolated from the silver sulfide mineral argyrodite (Ag_8GeS_6) and described by the German chemist Clemens Winkler (1886), who named it germanium, after his native country. More than one-half century elapsed after the isolation of germanium before its first commercial use in diodes and transistors was developed.

Germanium is a hard, brittle, grayish-white, semiconducting element that has electrical properties between those of a metal and an insulator. Germanium is metallic in appearance and has unique properties that make it critical to the function of numerous commercial, industrial, and military applications. It is consumed as a pure element or in compound form, depending on the application.

Indium

Indium was discovered in 1863 by German chemists Ferdinand Reich and H.T. Richter during a spectrographic analysis of sphalerite ore samples from Freiberg, Germany (Reich and Richter, 1863). They named the element indium after the distinctive indigo-blue line in its emission spectrum. Indium remained only a scientific curiosity for years following its discovery; little was known about its occurrence apart from the Freiberg ore.

Indium is a soft, lustrous, silvery-white metal with a low melting point relative to other metals. It is ductile and malleable, even at cryogenic temperatures; it has high wettability when melted and is resistant to thermal fatigue.

Uses and Applications

Germanium

Multiple stages of the germanium production process yield germanium compounds and metals that are designed for specific applications. Concentrated germanium is chlorinated and distilled to form the first usable product in the refining process, germanium tetrachloride ($GeCl_4$), which is a colorless liquid that is used primarily as a reagent in the production of fiber-optic cable. Germanium tetrachloride can be hydrolyzed and dried to produce germanium dioxide (GeO_2), which is another commonly used compound. Germanium dioxide is a white powder that is used to manufacture certain types of optical lenses and as a catalyst in the production of plastic polyethylene terephthalate (PET) resin.

Germanium dioxide can be reduced with hydrogen to produce a germanium metal powder, which is subsequently melted and cast into first-reduction bars. The germanium bars are then zone-refined (a process that involves melting and cooling germanium bars to isolate and remove impurities and ultimately yield extremely pure germanium) to produce electronic-grade germanium metal. Zone-refined germanium metal can then be grown into crystals and sliced for use as semiconductors or recast into forms suitable for lenses or window blanks in infrared optical devices (Bleiwas, 2010).

Germanium owes its usefulness to at least five salient properties. First, it is an intrinsic semiconductor, which in the pure state—that is, in the absence of contaminant elements in its crystal structure—will conduct electricity, albeit poorly. It is particularly effective as a conductor at high frequencies and low operating voltages. Second, germanium is transparent to part of the infrared electromagnetic spectrum, whether in the crystalline or glassy states. Third, like silicon, germanium is a glass-former, able to form extended three-dimensional networks of more or less randomly ordered germanium-oxygen tetrahedra. Fourth, it has an exceptionally high refractive index. Fifth, it exhibits low chromatic dispersion. These five properties, singly and sometimes in combination, determine the usefulness of germanium in electronics devices, night vision devices, fiber-optic cable, optical lens systems, and solar power arrays. A sixth property, of specific value to plastic bottle and container manufacturing—a single but commercially important use—is the ability of germanium to catalyze the polymerization of the plastic PET resin without undesirable coloring of the plastic product.

Germanium is relatively strong and is easily machined into infrared lenses and windows for infrared optical devices. Infrared imaging devices are used extensively by the military and law-enforcement agencies for surveillance, reconnaissance, and target-acquisition applications. Infrared optical devices improve a soldier's ability to operate weapon systems in harsh conditions effectively, and they are increasingly used in remotely operated unmanned weapons and aircraft. Infrared optical devices are also used for border patrol and by emergency response teams for conducting search-and-rescue operations.

Germanium substrates are used to form the base layer in multijunction solar cells, which are the highest efficiency solar cells currently available. The substrates are produced from high-purity, single-crystal germanium ingots that are sliced into wafers and polished. Ultrathin layer combinations of materials are "grown" on top of the germanium substrate, and each layer captures a specific part of the solar spectrum and converts it into electricity. These multijunction cells are the preferred type for use in space-based solar power applications because of their high energy-conversion efficiency and strength at minimal size (fig. I1).

Terrestrial-based photovoltaic installations are a potential growth area for germanium use (Bleiwas, 2010). Solar

powerplants that use concentrator technology composed of lenses or mirrors that focus high concentrations of direct sunlight onto germanium-based multijunction solar cells have emerged as viable sources for large-scale renewable energy generation. Germanium substrates are also used in high-brightness light-emitting diodes (LEDs) for backlighting liquid crystal display televisions and in vehicle headlights and tail lights.

Germanium tetrachloride is used to manufacture fiber-optic cables. Germanium is added to the pure silica glass core of the fiber-optic cable to increase its refractive index and minimize signal loss over long distances. Global demand for fiber-optic cable has increased significantly in recent years as technological advances have required ever-increasing bandwidth to transmit and receive data.

The major end uses for germanium worldwide are estimated to be fiber-optic systems (30 percent), infrared optics (25 percent), polymerization catalysts (25 percent), electronics and solar electric applications (15 percent), and other uses, including for chemotherapy, metallurgy, and phosphors (5 percent) (fig. I2*A*). The domestic end-use distribution is different and is estimated to be infrared optics (50 percent), fiber-optic systems (30 percent), electronics and solar electric applications (15 percent), and other uses, including for chemotherapy, metallurgy, and phosphors (5 percent) (Guberman, 2013a). Germanium is not used in polymerization catalysts in the United States.

Figure I1. Photograph of a concentrator photovoltaic (CPV) solar power system which, in 2013, earned a National Renewable Energy Laboratory (NREL) outdoor efficiency rating of 34.9 percent under international standard operating test conditions for concentrator photovoltaics—a new world record. Solar powerplants such as this that use lenses or mirrors to focus high concentrations of direct sunlight onto germanium-based multijunction solar cells have emerged as viable sources for large-scale renewable energy generation (Bleiwas, 2010; BusinessWire, 2013). Photograph courtesy of Arzon Solar, LLC.

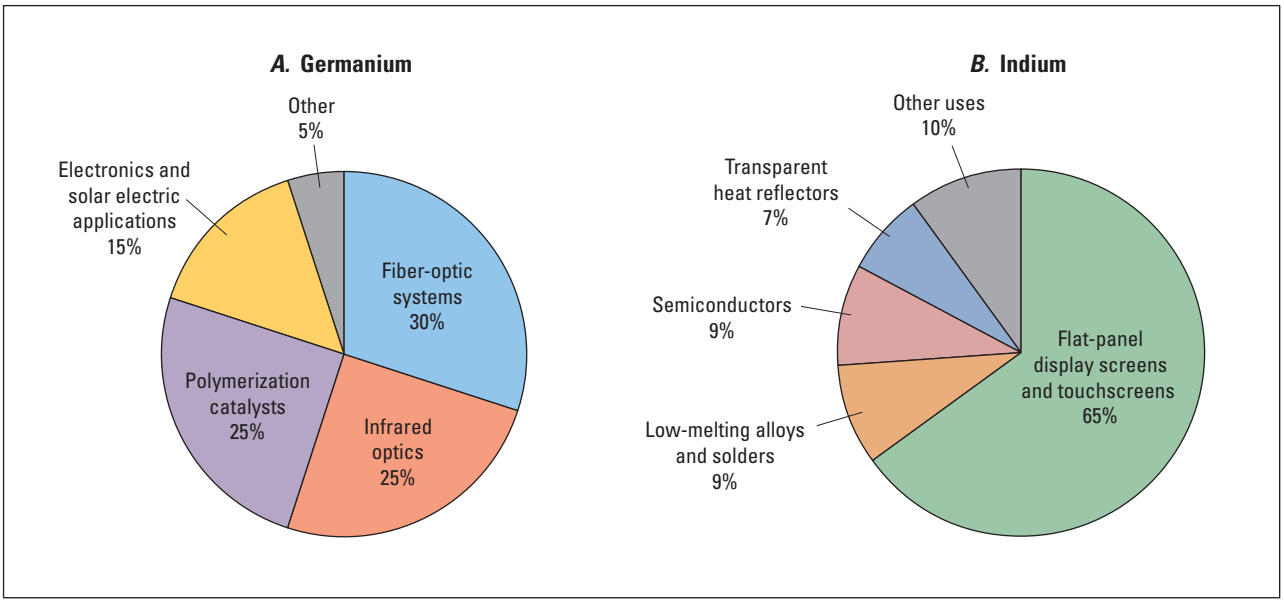

Figure I2. Pie charts showing major end uses of *A*, germanium and *B*, indium as a percentage of world consumption in 2012. Data are from Guberman (2013a) and Tolcin (2013a).

Indium

Indium metal with purities of up to 99.99995 percent is converted to different shapes and forms that have different uses. High-purity indium metal ingots are commonly used to produce indium compounds; indium shot is used in vapor deposition and plating applications; and indium wire, ribbon, and foil are typically used for soldering.

Indium is consumed mostly (65 percent) for the production of tin-doped indium oxide (or indium-tin oxide [ITO]), which is a transparent conducting oxide used in virtually every flat-panel display screen and touchscreen (figs. I2*B* and I3). ITO is typically deposited as a thin-film coating on the display surface, where it transforms incoming electrical data into an optical form. Most ITO production is concentrated in Japan, although significant quantities are also produced in China, the Republic of Korea, and Taiwan.

Alloys and solders are the second-ranked end use of indium globally (9 percent). Indium-containing solders have lower crack propagation and improved resistance to thermal fatigue compared with tin-lead solders. Indium-containing solders also inhibit the leaching of gold components in electronic apparatus. Certain types of indium alloys can be used as bonding agents between nonmetallic materials, such as glass, glazed ceramics, and quartz. Indium also is used in dental alloys and in white-gold alloys. Other indium alloys have been used as a substitute for mercury and in nuclear control rods.

Another important use of indium is in semiconductor materials for LEDs and laser diodes (9 percent). Indium antimonide, indium arsenide, or indium phosphide can be used as the substrate for indium-based semiconductors, and several indium-containing compounds can be used as the epitaxial layer (or substrate coating), such as indium-gallium-arsenide. Indium-based LEDs are used predominantly to transmit data optically and, to a lesser extent, in LED displays. Indium-based laser diodes are used in fiber-optic communications.

Demand and Availability of Supply

Substitutes for Germanium and Indium

Germanium.—Silicon can be a less-expensive substitute for germanium in certain electronic applications. Some metallic compounds can be substituted in high-frequency electronics applications and in some LED applications. Zinc selenide and germanium glass substitute for germanium metal in infrared applications systems but commonly at the expense of performance. Titanium has the potential to be a substitute as a polymerization catalyst.

Indium.—The indium-containing compound ITO, which is used as the transparent conducting film in many flat-panel display screens and touchscreens, has few substitutes. Various groups, however, have recently explored using antimony tin oxide, carbon nanotube coatings, and a number of other compounds to substitute for ITO in flat-panel and flexible display screens (Tolcin, 2013a).

Figure I3. Photographs showing *A*, indium-tin oxide (ITO), which is a transparent conducting oxide, and *B*, examples of flat-panel display screens and touchscreens. ITO is typically deposited as a thin-film coating on the display surface where it transforms incoming electrical data into an optical form. Photograph *A* courtesy of Indium Corp.; photograph *B* courtesy of CI Systems, Inc.

Strategic and Critical Resource Issues

Germanium.—The extensive use of germanium for military and commercial applications has made it a critical material in the United States and the rest of the world. Germanium was included in the National Defense Stockpile in 1984 and was more recently added to a stockpile program in China. In 2010, the European Union included germanium in a list of raw materials of critical concern for its member countries owing to its expected economic importance and relative supply risk (European Commission, 2010).

Few adequate substitutes exist for germanium for applications that are important for defense and law enforcement, such as infrared optics and substrates for solar cells in satellites. Most germanium production is concentrated in a few countries—Canada, China, Finland, and Russia. The United States is dependent on imports for its germanium consumption. As a byproduct metal, the supply of germanium is heavily reliant on zinc production. It has been estimated that less than 5 percent of the germanium contained in zinc concentrates reaches refineries that are capable of extracting and producing germanium.

Indium.—Indium can be considered a critical material for display technology because there are few substitutes. Because indium is recovered as a byproduct of zinc production, the supply of primary indium is determined by the supply of zinc, regardless of the market demand for indium. Additionally, a large portion of the indium contained in zinc ores and concentrates is not recovered—most zinc smelters are not equipped to extract indium. At the few smelters that do include indium-processing circuits, the average indium recovery rate is only about 50 percent (ranging from 30 to 80 percent) (Jorgenson and George, 2004). Increased consumption of indium is expected to be satisfied by increased recycling and additional primary supply through improved recovery rates, the construction of new plants, and expansions at existing recovery circuits (Alfantazi and Moskalyk, 2003).

Geology

Geochemistry

Germanium.—Germanium has a crustal abundance of 1.6 parts per million (ppm), making it about the 50th most abundant element. In elemental form, germanium is a hard, gray-white metalloid with an atomic number of 32. It is a Group 4A element in the periodic table and has properties similar to its neighbors silicon and tin. Germanium most commonly exists in the +4 and +2 valence states and commonly substitutes for silicon or tin.

Aqueous germanium (as Ge^{4+}) forms complexes with fluoride, hydroxide, phosphate, and sulfate in low-temperature environments. At hydrothermal temperatures (up to 300 degrees Celsius [°C]), the principal complex is germanic acid (H_4GeO_4), but germanium-fluoride complexes may be important at high-fluorine concentrations (Wood and Samson, 2006). Germanium concentrations of up to about 300 parts per billion (ppb) have been reported for some geothermal waters (Höll and others, 2007). Further evidence for hydrothermal transport comes from germanium concentrations of up to 20 ppm in hydrothermal sinter deposits in New Zealand geothermal systems (Krupp and Seward, 1987) and of up to about 270 ppm in modern sea-floor hydrothermal sulfide deposits (Bischoff and others, 1983).

Indium.—Indium has an average crustal abundance of about 49 ppb and is the 61st most abundant element. Elemental indium is very soft, lustrous, metallic, and malleable, and it has a very low melting point of 156.6 °C. It is a Group 3A element in the periodic table and has chemical properties similar to its group neighbors gallium and thallium. Indium most commonly occurs in the +3 valence state.

Schwarz-Schampera and Herzig (1999) reported indium concentrations of up to 590 ppm in modern sea-floor hydrothermal sulfide deposits of the Valu Fa Ridge in the Lau Basin of the western Pacific Ocean, so indium clearly is transported and deposited in hydrothermal systems. Seward and others (2000) experimentally determined that indium is complexed by chloride in aqueous solutions at temperatures of up to 350 °C.

Chaplygin and others (2007) have shown that abundant indium—of up to 4.75 weight percent in sphalerite—occurs at fumaroles of the Kudriavy volcano on Iturup Island in the Kuril Islands, Russia. The fumarole deposits form at 400 to 750°C, showing that vapor transport in high-temperature systems is also possible.

Mineralogy

Germanium.—Germanium can occur as the following rare minerals (with approximate compositions): argyrodite (Ag_8GeS_6), germanite ($Cu_{13}Fe_2Ge_2S_{16}$), renierite ($(Cu,Zn)_{11}(Ge,As)_2Fe_4S_{16}$), or briartite ($Cu_2(Fe,Zn)GeS_4$). Germanium is primarily recovered as a byproduct from zinc, silver, lead, and copper ores, however. Laser ablation and inductively coupled plasma-mass spectrometry (ICP–MS) traverses across minerals by Ye and others (2011) have shown that germanium occurs in true solid solution in sulfide minerals and is most strongly enriched in sphalerite from Mississippi Valley-type (MVT) deposits, which are strata-bound, carbonate-hosted lead-zinc deposits that form epigenetically from basinal brines at low to moderate temperatures (typically 150 to 225 °C).

Indium.—Indium forms a few minerals, such as dzhalindite ($In(OH)_3$) and indite ($Fe^{+2}In_2S_4$), but is not found concentrated into significant deposits. Indium is primarily produced as a byproduct from zinc ores. Ye and others (2011) provide evidence that indium, like germanium, is in true solid solution in sphalerite.

Deposit Types

Germanium

Germanium does not form specific deposits, but rather occurs as a byproduct in a variety of deposit types that contain copper, gold, lead, silver, and zinc. Germanium concentrations in sphalerite from these deposits are typically a few hundred parts per million. Because byproduct production comes from metallurgical operations that are commonly fed by concentrates from any number of different deposits and locations, it is difficult to track germanium production back to a specific deposit. The example deposits discussed below, however, are known to be significant contributors to major germanium-producing facilities.

Types of deposits that contain significant germanium include volcanogenic massive sulfide (VMS) deposits, sedimentary exhalative (SEDEX) deposits, Mississippi Valley-type (MVT) lead-zinc deposits (including Irish-type lead-zinc deposits), and Kipushi-type zinc-lead-copper replacement bodies in carbonate rocks (table I1; Höll and others, 2007). Germanium is most enriched in the Kipushi-type deposits, but worldwide production is mostly from low-temperature stratiform sphalerite deposits (where mineralization follows stratigraphic layering) and strata-bound sphalerite deposits (where mineralization may cross-cut strata but is restricted to a particular stratigraphic unit).

Sedimentary exhalative deposits.—The Red Dog zinc-lead-silver mining district (fig. I4) in the western Brooks Range of northern Alaska contains several zinc-lead-silver sulfide bodies and prospects separated into thrust fault slices (Johnson and others, 2015). The four primary deposits of the Red Dog Mine have reserves and resources totaling 141 million metric tons at grades of 16.6 weight percent zinc and 4.6 weight percent lead (Jennings and King, 2002). The deposits are hosted in the Mississippian Kuna Formation black shales and mudstones that were deposited in a closed extensional basin that experienced euxinic conditions (Johnson and others, 2015).

Kelley and others (2004) showed that the deposits in the Red Dog district have a complex paragenetic history that they divide into four stages: (1) shallow subsurface impregnation of unconsolidated muds with abundant barite ($BaSO_4$) and early brown sphalerite, (2) subsea-floor deposition of yellow-brown sphalerite with barite, (3) deposition of red-brown sphalerite, and (4) faulting and tectonic brecciation accompanied by deposition of late tan sphalerite. Kelley and others (2004)

Table I1. Classification of deposits that host germanium and indium resources.

[Elements: Ag, silver; As, arsenic; Au, gold; Ba, barium; Be, beryllium; Bi, bismuth; Cd, cadmium; Co, cobalt; Cr, chromium; Cu, copper; Fe, iron; Ga, gallium; Ge, germanium; Hg, mercury; In, indium; Mn, manganese; Mo, molybdenum; Ni, nickel; Pb, lead; PGE, platinum-group elements; Re, rhenium; Sb, antimony; Se, selenium; Sn, tin; Te, tellurium; Tl, thallium; U, uranium; W, tungsten; Zn, zinc]

Deposit type	Short name	Characteristics	Metals present (and source of information)
Volcanogenic massive sulfide deposits	VMS	Stratiform Cu-Pb-Zn sulfide deposits in submarine mafic to felsic volcanic terranes that form at the sea floor by venting of hydrothermal fluids driven by magmatic heat and volatiles	Cu-Zn-Pb-Au-Ag with Be, Bi, Cd, Co, Cr, Ga, Ge, Hg, In, Mn, Mo, Ni, Se, Sn, Te, and PGE (Shanks and Thurston, 2010)
Sedimentary exhalative deposits	SEDEX	Stratiform, often finely laminated, Zn-Pb-Ag sulfide deposits in carbonaceous and pyrite shales and siltstones that form by exhalation of hydrothermal fluid on the sea floor without any direct igneous association	Zn-Pb-Ag with As, Bi, Cd, Co, Cu, Ga, Ge, Hg, In, Mn, Ni, Sb, Se, Sn, and Tl (Goodfellow and Lydon, 2007; Kelley and others, 2004; Slack and others, 2004)
Mississippi Valley-type Zn-Pb deposits	MVT	Strata-bound epigenetic Zn-Pb sulfide replacement deposits along faults and permeable zones and open-space fill in solution collapse breccias in dolostone and limestone. Not associated with igneous activity	Zn-Pb with Cu, Ni, and Co (Leach and others, 2005)
Kipushi-type Zn-Pb-Cu replacement bodies in carbonate rocks	Carbonate replacement deposits (CRD)	Strata-bound epigenetic Zn-Pb-Cu sulfide ore deposits in irregular pipe-like bodies associated with collapse breccias and faults as well as lenticular bodies subparallel to the bedding. Association with igneous activity is unclear	Zn-Pb-Cu with Ag, As, Bi, Cd, Co, Ga, Ge, Mo, Re, Sb, Sn, and W (Kampunzu and others, 2009)
Polymetallic Zn-Sn vein and fissure-filling deposits	Polymetallic vein deposits	Polymetallic sulfide veins forming dense arrays in volcanic rocks, eroded volcanic-intrusive complexes, porphyry stocks, and associated breccia	Zn-Cu-Pb-Sn-In with Ag, As, Bi, Co, Ga, Mn, Ni, Sb, Se, and W (Ishihara and others, 2011)
Coal and lignite deposits	None	Ge concentrated in organic matter of coal seams that have been affected by hydrothermal activity and are generally associated with siliceous layers	Ge in coal with As, Ba, Sb, U, and W

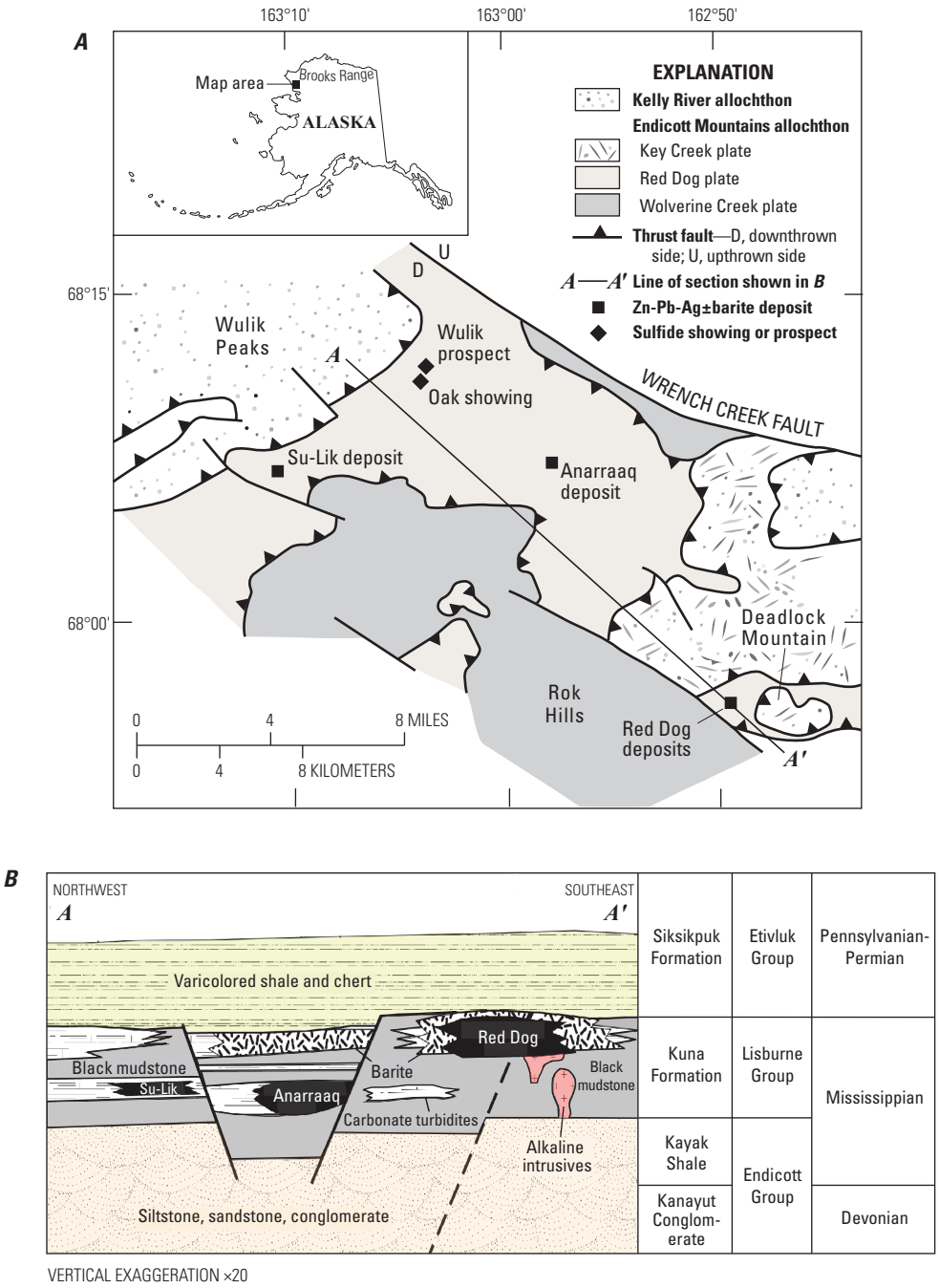

Figure I4. Map and schematic cross section showing the geology of the Red Dog mining district in Alaska and the stratigraphy of selected deposits in the district. *A*, Simplified geology of the Red Dog district in the western Brooks Range, Alaska, and the locations of major zinc-lead-silver (Zn-Pb-Ag) ± barite deposits. The exposure is distal to known sulfide deposits, but sulfide showings have been identified nearby. Modified from Johnson and others (2015), De Vera and others (2004), and Young (2004). *B*, Stratigraphic positions of Zn-Pb-Ag sulfide deposits and barite deposits in the Red Dog district. This geologic section has Jurassic-Cretaceous thrust faulting removed, so the structural plates above the Red Dog plate are not shown and originally underlying strata have been restored. Modified from Johnson and others (2015) and Kelley and Jennings (2004).

further show that sphalerite from all four stages is enriched in germanium and that the average concentrations range from 104 to 249 ppm. The highest germanium values occur in low-iron, lower temperature, late tan sphalerite. Most of the germanium produced at metallurgical facilities at Trail, British Columbia, Canada, likely comes from sphalerite concentrates from the Red Dog district.

The Fankou lead-zinc deposit in Guandong Province, China, is a carbonate-hosted strata-bound deposit hosted in Devonian to Carboniferous carbonates and shales (Höll and others, 2007). Gu and others (2007) cite evidence for the classification of the Fankou deposit as SEDEX with both stratiform and cross-cutting mineralization. Since mining began in the 1960s, the Fankou Mine has produced 150,000 metric tons of lead-zinc sulfide containing about 15 weight percent lead and zinc combined; the sulfide is also enriched in sphalerite that contains from 30 to 170 ppm germanium (Xuexin, 1984; Höll and others, 2007).

Irish-type carbonate-hosted lead-zinc deposits have characteristics of both MVT and SEDEX deposits. The Silvermines–Lisheen group of deposits in the Midlands basin of County Tipperary, Ireland, formed by replacement of lower Carboniferous carbonate sediments near the sea floor and represent potentially important deposits of germanium. Wilkinson and others (2005) reported that microprobe analysis of minerals from drill core samples of the Lisheen deposit determined the germanium concentrations to be 400 to 900 ppm in sphalerite, 200 to 1,300 ppm in galena, and 200 to 1,000 ppm in tennantite ($(Cu,Fe)_{12}As_4S_{13}$). Despite these favorable reports, no production of byproduct germanium was reported by Vedanta Resources plc of India, which owned the Lisheen deposit.

Mississippi Valley-type deposits.—The Gordonsville-Elmwood zinc-lead district in Tennessee hosts examples of zinc-rich MVT deposits that formed in collapse breccias related to large cavernous underground areas; these deposits, on average, have grades of about 400 ppm germanium in zinc ore concentrate (Misra and others, 1996). Other MVT deposits in the United States average about 50 ppm germanium in sphalerite. The Gordonsville Mine near Nashville, Tennessee, has produced 45,000 metric tons per year of zinc, and byproduct germanium production has been significant. In 2010, Nyrstar N.V. of Switzerland reopened the zinc mines in the Carthage mineral district in Tennessee, which includes the Elmwood, Gordonsville, and Cumberland Mines (Nyrstar N.V., 2016). The company reported production of 109,000 metric tons of zinc concentrate from these mines in 2012; the concentrates were processed at Nyrstar's Clarksville, Tenn., roast leach electrowin smelter complex, which produced a germanium concentrate as well as cadmium metal, copper sulfate, sulfuric acid, synthetic gypsum, and zinc metal (Nyrstar N.V., 2013, p. 6, 23).

The Huize MVT deposit, which is located in Carboniferous dolomites and limestones of China's eastern Yunnan Province (fig. I5), is one of the largest MVT deposits in China. The Huize Mine produces, in order of abundance, zinc-lead and byproduct silver, germanium, and cadmium (fig. I5; Ye and others, 2011).

Kipushi-type Zn-Pb-Cu replacement bodies in carbonate rock.—The most significant carbonate-hosted zinc-lead-copper deposits that contain notable amounts of germanium are the Kipushi deposit in the Democratic Republic of the Congo (Congo [Kinshasa]) and the Kabwe deposits in Zambia (fig. I6; Kampunzu and others, 2009). Kipushi-type deposits are strata-bound irregular pipelike sulfide bodies in platform carbonate rocks. Collapse breccias, faulting, and stratiform lensoidal sulfide bodies are commonly associated with Kipushi-type deposits. The Kipushi deposit is hosted in the upper Katangan Kundelungu Group (760 to 565 mega-annum [Ma]) that consists of alternating carbonate rocks, shales, and sandstones. Schneider and others (2007) report concordant ages of 451.1±6.0 Ma and 450.5±3.4 Ma from direct rubidium-strontium and rhenium-osmium isochron dating, respectively, of ore-stage zinc-copper-germanium sulfides. Further, this age of ore formation indicates that mineralization is related to crustal fluids related to Ordovician extension.

Germanium averages 68 ppm in bulk samples in the Kipushi deposit and occurs substituted in sulfide minerals, although it sometimes occurs in separate copper-iron-germanium sulfide minerals. The actual amount of byproduct germanium production from mining is unknown.

Coal and lignite deposits.—China is a major producer of germanium from coal. The Lincang lignite mine, which is located close to Lincang City in Yunnan Province, is a significant source of germanium; the mine produces 16 metric tons of high-grade germanium dioxide (GeO_2) annually, of which 90 percent is exported (fig. I5; Höll and others, 2007). Germanium is produced at the Lincang Mine from a lower lignite unit that is close to the contact with germanium-rich granitic rocks below. Hu and others (2009) report that the Lincang deposit contains 1,000 metric tons or more of germanium at a grade of 850 ppm. Germanium-rich coal seams are interbedded with siliceous rocks, including siliceous limestones, whereas other nearby seams that do not have the association with siliceous rocks are barren of germanium. The siliceous rocks have oxygen and carbon isotope characteristics that suggest a hydrothermal origin. Hu and others (2009) propose that hydrothermal fluids first leached germanium from granitic rocks. The fluids were then discharged as hot springs along fault zones into Miocene basins where the germanium was concentrated in lignite seams within stratiform siliceous and siliceous-limestone deposits.

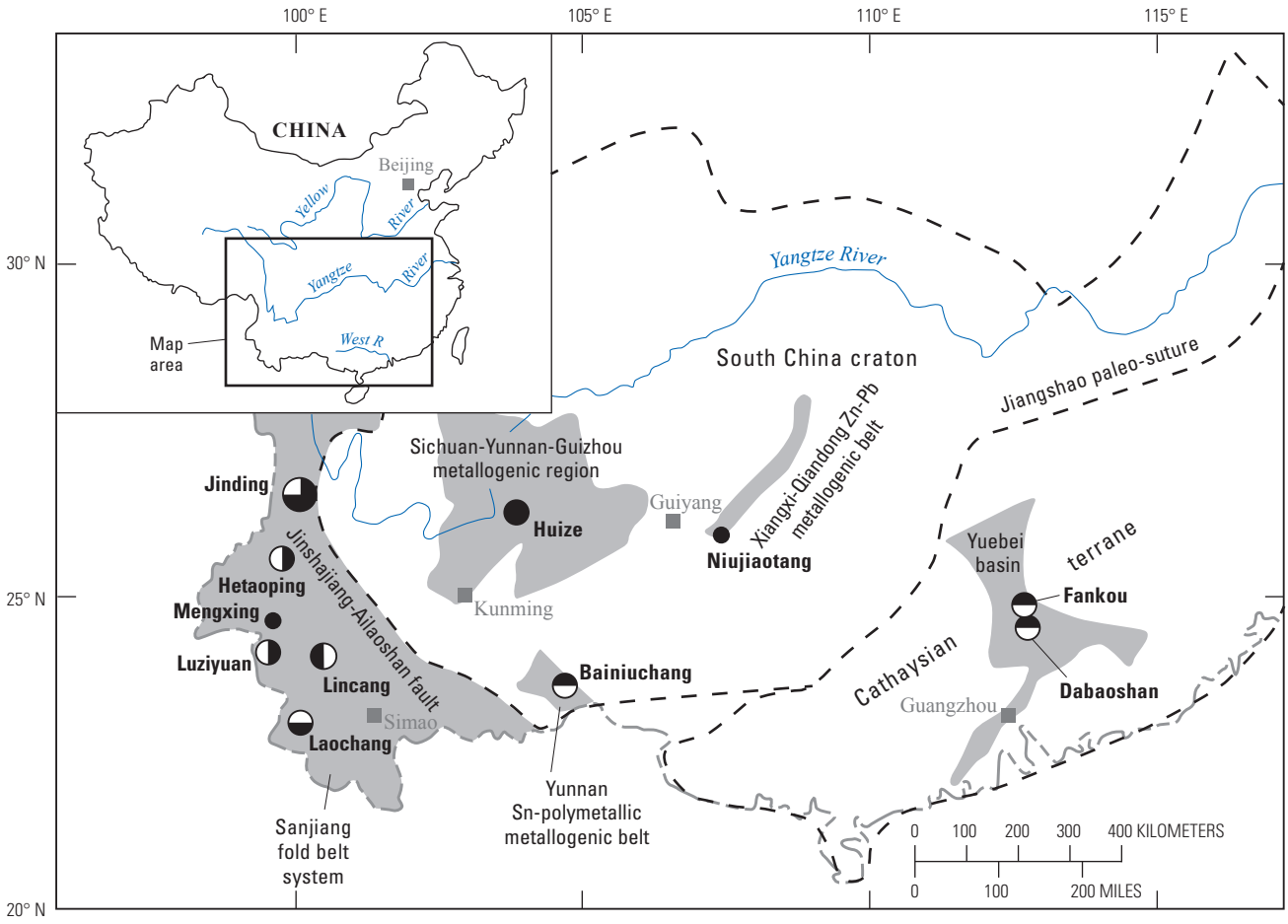

Figure I5. Map showing the locations and geologic settings of selected volcanogenic massive sulfide (VMS), sedimentary exhalative (SEDEX), Mississippi Valley-type (MVT), and coal (lignite) deposits and other types of deposits in southern China. Modified from Ye and others (2011). Pb, lead; Sn, tin; Zn, zinc

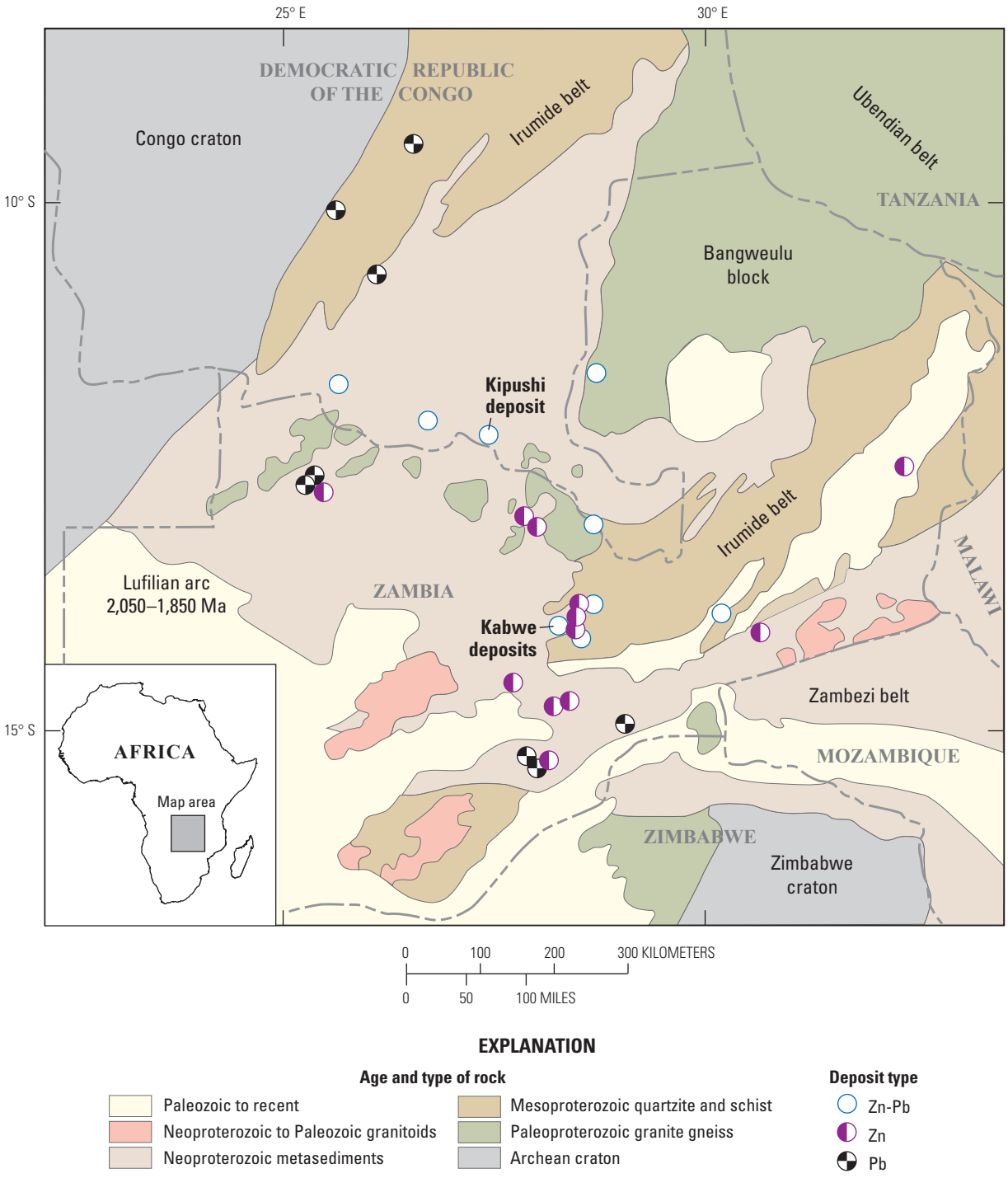

Figure I6. Map showing the location of Kipushi-type deposits (including the Kabwe deposits) and major Neoproterozoic orogenic belts and basins in the Precambrian tectonic framework of southern Africa. Modified from Kampunzu and others (2009). Pb, lead; Zn, zinc

Indium

Approximately one-half of the byproduct indium in the world is produced at smelters located in southern China, but the Republic of Korea, Japan, Canada, Belgium, and Peru (in order of output) also produce significant byproduct indium. More than one-half of the material for the smelters in China comes from VMS and SEDEX deposits, and much of the remaining production comes from MVT deposits. It is difficult to decipher which VMS, SEDEX, and MVT deposits in the world provide the zinc feedstock processed at the Chinese smelters, however.

Volcanogenic massive sulfide deposits.—The Laochang deposit in Yunnan Province, China (fig. I5), and the VMS deposits of the Murchison greenstone belt in Limpopo Province, South Africa, provide excellent examples of indium-enriched VMS deposits. The Laochang deposit, which is hosted by a lower Carboniferous volcano-sedimentary sequence, occurs at the junction between southeast- and northwest-trending basement faults. Sphalerite samples analyzed by Ye and others (2011) have indium contents of up to 544 ppm but average about 200 ppm.

The dozen or so VMS deposits of the Archean Murchison greenstone belt in South Africa occur in a felsic volcanic back-arc basin that was accreted to a continental margin (Schwarz-Schampera and others, 2010; Zeh and others, 2013). The VMS deposits typically consist of lower temperature zinc-rich sea-floor sulfide mineralization that, in some cases, is overprinted by higher temperature copper-rich mineralization. Indium is closely associated with copper-rich ores, and indium concentrations range from 24 to 641 ppm in the Maranda J, Romotshidi, and Solomons deposits of the Murchison greenstone belt (Schwarz-Schampera and others, 2010).

Sedimentary exhalative deposits.—The SEDEX deposit at Bainiuchang, China, is located in southeastern Yunnan Province (fig. I5). Mineralization occurs in stratiform massive sulfide lenses in mid-Cambrian dolomite, limestone, and sandstone. Indium in sphalerite at Bainiuchang averages 71 ppm but shows large fluctuations, from 4 to 262 ppm (Ye and others, 2011).

The Dabaoshan SEDEX deposit is located in the Nanling region of China and occurs at the contact between Devonian argillaceous limestones and underlying sandstones and shales (fig. I5). The deposit contains about 40 lenses of zinc-lead ore, and pyritic copper zones occur on the margins of some lenses. Indium in sphalerite of the Dabaoshan deposit averages 300 ppm and shows little variation in the samples studied by Ye and others (2011).

Polymetallic tin vein deposits.—Polymetallic tin deposits of Bolivia (including the Bolívar, Hauri Hauri, Porco, Potosí, and San Lorenzo deposits, and others) constitute a major potential source of indium. Total indium metal resources in the Bolivian polymetallic tin deposits are estimated to be 12,000 metric tons (Ishihara and others, 2011). The polymetallic tin belt that occurs in the Eastern Cordillera of the Andes Mountains of Bolivia (Ishihara and others, 2011) is underlain by Paleozoic marine sedimentary rocks overlain and intruded by Cenozoic felsic volcanic and intrusive rocks that are associated with the mineralization (fig. I7). Deposits occur as dense arrays of narrow, elongate zinc sulfide and cassiterite (SnO_2) veins that occur in volcanic rocks, eroded volcanic-intrusive complexes, porphyry stocks and associated breccia, and Paleozoic sedimentary rocks. Individual Bolivian polymetallic tin deposits have indium contents in composite ore samples or zinc concentrates of 584 ppm at Bolívar, 3,080 ppm at Hauri Hauri, 499 ppm at Porco, 292 ppm at Potosí, and 1,080 ppm at San Lorenzo (Ishihara and others, 2011; Murakami and Ishihara, 2013).

Mining and Beneficiation Methods

Germanium.—Germanium is initially recovered from the leaching of zinc residues or coal ash followed by precipitation of a germanium concentrate. The extraction of germanium from its ores includes two stages—the production of a germanium concentrate by retorting, roasting, or pyrometallurgy and deposition of germanium sulfide or oxide. Concentrates are chlorinated to germanium tetrachloride ($GeCl_4$) and subsequently purified by hydrolysis to germanium dioxide (GeO_2), reduced pyrolytically with hydrogen gas (H_2) to germanium metal powder, and melted into bars (Butterman and Jorgenson, 2005).

Indium.—Indium is recovered as a byproduct during the refining process of other base-metal ores and concentrates, most commonly the zinc ore mineral sphalerite. Several complex and proprietary methods have been developed to extract indium from different source materials; however, a generalized recovery process is described, as follows, by Alfantazi and Moskalyk (2003). Waste products generated during the zinc refining process, such as dusts, fumes, residues, and slag, are collected and treated for the recovery of indium. These materials are first leached with hydrochloric or sulfuric acid to dissolve the indium into an aqueous solution. The solution then undergoes a solvent extraction process to increase the concentration of indium in the solution. Next, indium is removed from the solution by means of cementation, and the resulting indium sponge is cast into anodes for electrolytic refining to produce indium metal of standard-grade purity (99.97 or 99.99 percent).

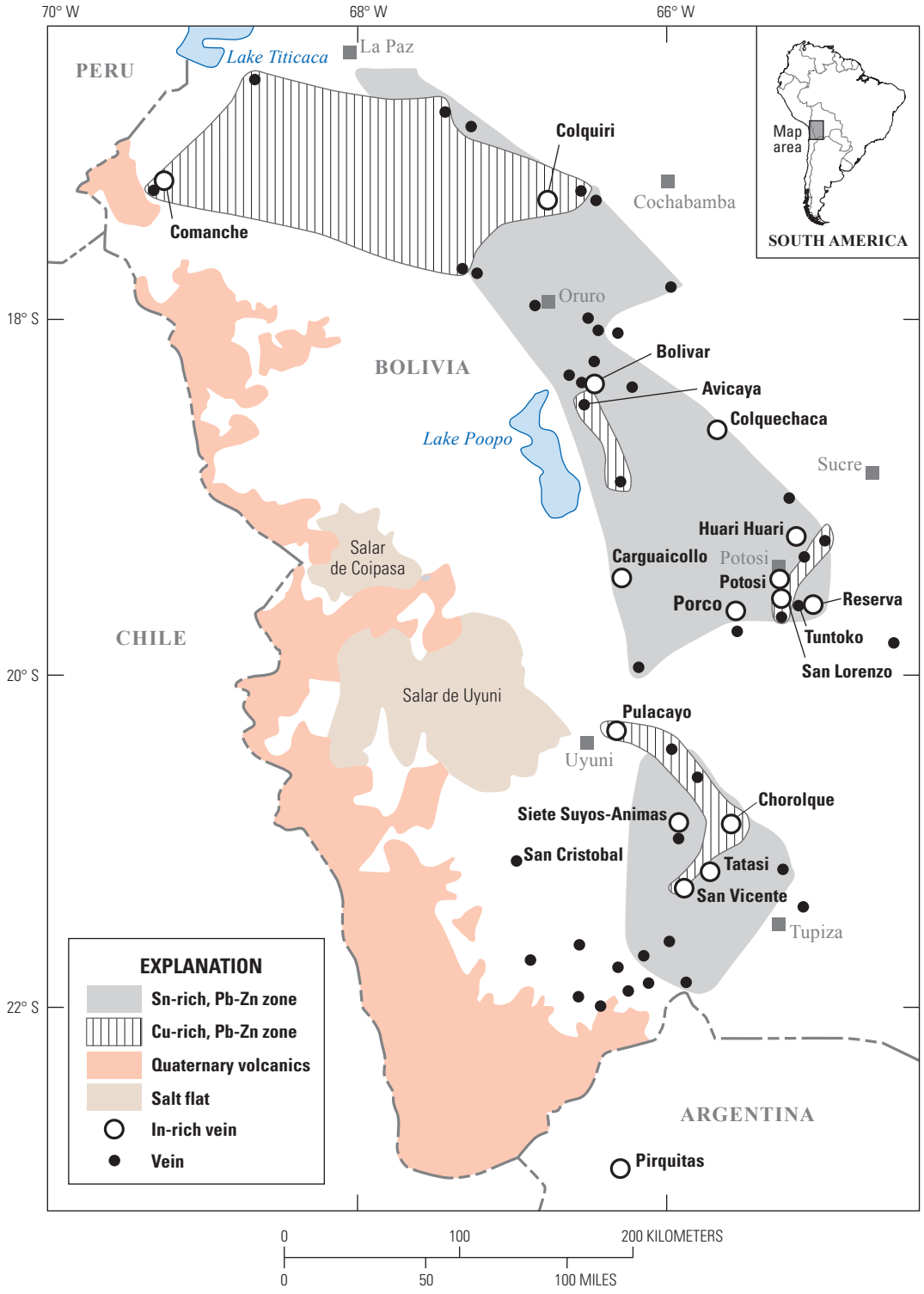

Figure I7. Map showing indium-bearing tin-polymetallic ore deposits in Bolivia. Modified from Ishihara and others (2011); copper-rich zone is from Schwarz-Schampera and Herzig (2002). Cu, copper; In, indium; Pb, lead; Sn, tin; Zn, zinc

Resources and Production

Reserves, Other Identified Resources, and Undiscovered Resources

Estimating reserves of either germanium or indium is difficult because they are byproduct commodities that come from a wide variety of ore deposit types. For example, both germanium and indium come largely from the zinc ore mineral sphalerite. Global zinc reserves are estimated to be 250 million metric tons, and domestic U.S. reserves are estimated to be 11 million metric tons. Accurately converting these values to reserves for germanium or indium would require an intensive program of chemical analyses for these elements in sphalerite, and there are insufficient data available to calculate average concentrations in all the relevant deposits, which is a necessary step in determining reserves. Guberman (2013a) estimated U.S. reserves for germanium to be 450 metric tons.

Germanium and indium are closely associated with currently produced zinc, copper, and tin-polymetallic ores, and coal deposits (Weeks, 1973; Schwarz-Schampera and Herzig, 2002; Höll and others, 2007; Bleiwas, 2010). Much of the ore that might provide byproduct germanium and indium currently is processed without separation of these constituents. The extent of recovery in the future will depend on (a) a continued increase in demand for indium and germanium, (b) better metallurgical recovery technology from sulfides and other materials, and (c) careful implementation of recycling of electronic products and production waste. Ores of metals other than zinc (especially some copper-tin ores), coal deposits, and fly ash from coal burning, have potential significant concentrations of germanium and indium and might become important sources. It is unlikely that exploration for deposits containing germanium and indium will be conducted solely because the deposits contain these byproduct elements. Two deposits have been developed primarily for production of germanium or indium. The indium-producing Toyoha Mine in Hokkaido Prefecture, Japan, closed in 2006 and the germanium-producing Apex Mine in Utah closed in 1992.

The Toyoha Mine, which is a lead-zinc-silver-indium vein deposit located near Sapporo, Japan, was until recently the world's leading indium producer (30 metric tons per year), but the mine was closed when ore reserves were exhausted. The deposit consists of a series of steeply dipping zinc-lead-silver-copper-tin-indium veins that occur across an area 500 meters (m) long and 2,500 m wide and has vein widths of up to 30 m. Total indium production from the Toyoha Mine was estimated to be 5,000 metric tons, based on an average indium grade of 138 ppm (Shimizu and Morishita, 2012).

The Apex Mine near Saint George, Utah, was the first mine in the world devoted primarily to production of gallium and germanium when it was reopened in 1986 (Bernstein, 1986). The Apex deposit was mined from 1884 to 1962 for copper, lead, and silver, which removed the copper-rich ores. Gallium and germanium mining after 1986 focused mainly on azurite, goethite, hematite, jarosite, limonite, malachite, and minor amounts of other metal arsenates, carbonates, oxides, and sulfates. These minerals occur in dolomitized and silicified breccia, gouge, and fissures in steeply dipping fault zones within the gently dipping Pennsylvanian Callville Limestone. Germanium is concentrated (up to 7,000 ppm) mostly in the goethite, hematite, and limonite (Bernstein, 1986). Reserves of 247,000 metric tons at an average grade of 1,000 ppm germanium were estimated in 1986 (Ludington and others, 2006). Production was reported as 2,555 kilograms of germanium in 1986 (Burgin, 1988, p. 485). Cox and Singer (1986) and Ludington and others (2006) consider the Apex deposit to be a Kipushi-type deposit.

Although deposit and mine development exclusively for germanium and indium is unlikely, two promising deposits that could be sources of production primarily for these minerals have recently been described. Ludington and others (2006) report small base-metal deposits in Paleozoic limestone in the Gold Butte area and the Tramp Ridge area in Clark County, Nevada. These are unlikely ever to be significant sources of copper, lead, silver, or zinc; however, they may contain potentially significant concentrations of gallium and germanium, as well as cobalt. The characteristics of these deposits indicate clearly that they can be considered to be Kipushi-type deposits (Ludington and others, 2006).

Another prospect of interest is the Crypto zinc-copper-indium project in Juab County, Utah, which contains copper and zinc skarn deposits in Paleozoic limestones (Nilsson and others, 2010). Indium concentrations average about 31 ppm, and indium resources are estimated to be about 475 metric tons of contained indium.

Production

Worldwide production of both germanium and indium has increased dramatically over the past several decades. Figure I8 shows the increases in global production since 1999 (Guberman, 2013a; Tolcin, 2013a). Production of each commodity in individual countries in 2011 and 2012 are discussed separately below.

Germanium.—In 2011, the world's total production of germanium was estimated to be 118 metric tons (table I2). This total includes germanium recovered from zinc concentrates, fly ash from coal burning, and recycled material. Worldwide, primary germanium was recovered in Canada from zinc residues (concentrates) shipped from the United States (specifically, the Red Dog zinc-lead mine in Alaska and a previously idled zinc mine complex in Tennessee); in China, from zinc residues and coal from multiple sources; in Finland, from zinc residues (concentrates) originating in Congo (Kinshasa); and in Russia, from coal from domestic sources on Sakhalin Island in Sakhalinskaya Oblast' (Höll and others, 2007). The vast majority of germanium production was concentrated in Canada and China (Bleiwas, 2010).

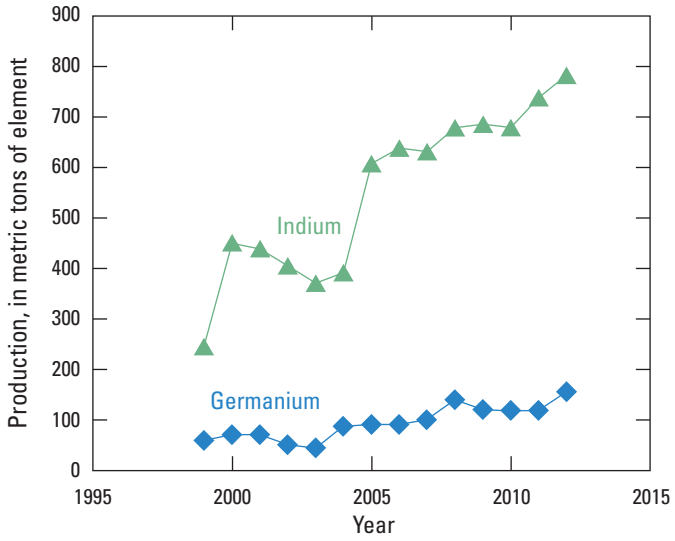

Figure I8. Graph showing worldwide production of germanium and indium from 1995 to 2012. Production of both minerals increased significantly. Graph was compiled using data from Jorgenson and George (2004), Guberman (2013a, b) and Tolcin (2013a, b).

Table I2. Average estimated annual refinery production of germanium and indium, by area, for 2011 and 2012.

[Sources: Guberman, 2013a, 2014; Tolcin, 2013a, 2014. W, withheld to avoid disclosing proprietary data; —, zero production; n.d., no data]

Country	Refinery production (metric tons)	
	2011	2012
Germanium		
United States	3	W
China	80	105
Russia	5	5
Other countries[1]	30	40
World total	**118**	**150**
Indium		
United States	—	—
Belgium	30	30
Brazil	5	n.d.
Canada	75	62
China	380	405
Japan	70	71
Korea, Republic of	70	165
Peru	n.d.	11
Russia	5	13
Other countries	27	25
World total	**662**	**782**

[1]Germanium production in Canada is substantial, but exact figures are proprietary, so Canadian production is included with "Other countries."

Owing to the value of refined germanium, new scrap generated during the manufacture of fiber-optic cables, infrared optical fiber, and substrates is typically reclaimed and fed back into the production process. Recycling of germanium recovered from used materials, such as fiber-optic window blanks in decommissioned military vehicles or fiber-optic cables, has increased during the past decade. A germanium refinery in Utica, New York, produces germanium tetrachloride for optical fiber production. Another refinery in Quapaw, Oklahoma, produces refined germanium compounds for the production of fiber optics, infrared devices, and substrates for electronic devices.

Indium.—Globally, primary production of indium metal in 2011 was estimated to be about 662 metric tons, of which about one-half was produced in China (table I2). Other leading producers were Belgium, Canada, Japan, and the Republic of Korea. These five countries accounted for almost 95 percent of primary indium production. Major production facilities outside of China included Teck Resources Ltd.'s Trail lead-zinc metallurgical complex in Canada, Korea Zinc Ltd.'s Onsan lead-zinc smelter in the Republic of Korea, Dowa Metals and Mining Co. Ltd.'s Akita zinc smelter in Japan, and Umicore NV's Hoboken precious-metals refinery in Belgium (Guberman, 2013a; Tolcin, 2013a).

In the United States, indium metal was not produced as a byproduct at any smelters or refineries. Domestic production of indium consisted of upgrading imported indium metal and powder. Indium Corp. of America and Umicore Thin Film Products accounted for the majority of U.S. production of indium metal and products.

Prices and Pricing

Germanium.—Germanium is traded through long-term supply contracts and individual trades between large consumers and suppliers as well as private trading houses. The terms of such trades are generally unavailable publicly, and a market price, in the conventional sense, does not exist. Publicly available price quotes actually represent estimates of representative prices in trades being executed on a particular day, which are compiled through recurring interviews with individual traders. Germanium prices have fluctuated on a regular basis owing to supply disruptions and increases in consumption of germanium for emerging applications. Germanium dioxide prices in 2012, for example, increased by 49 percent to $1,375 per kilogram in late September, up from $925 per kilogram in mid-March (Guberman, 2013a, b). Because germanium commonly is produced as a byproduct of zinc, the supply and price of germanium is often affected by the zinc market. Germanium metal trades at a significantly higher price than germanium dioxide, reflecting the value added and cost of this further refining.

Indium.—The average indium price in 2012 was $530 per kilogram. In 2011, indium prices fluctuated between a high of $785 at the beginning of the year and a low of $485 in July, ending the year at approximately $540 per kilogram (Tolcin, 2013a, b).

Environmental Considerations

Germanium and indium are becoming increasingly more important to society, given their increasing use in microelectronic applications. Compared with more-abundant industrial metals, such as lead and zinc, information about the behavior of germanium and indium in the environment is limited.

Sources and Fate in the Environment

In surface weathering environments, germanium and indium may dissolve from host minerals and form complexes with chloride, fluoride, hydroxide, organic compounds, phosphate, or sulfate. In dissolved form, germanium and indium most often occur in the +4 and +3 oxidation states, respectively (Wood and Samson, 2006). The behavior of germanium in weathering environments mirrors that of silicon, so measurement of germanium-to-silicon ratios in diatoms (single-celled alga with a cell wall of silica) in rivers and oceans has been used as a tool to document weathering of silicate rocks through geologic time (for example, Froelich and others, 1992). Indium has no equivalent relationship with another element in weathering environments, but it does tend to co-precipitate with iron and manganese oxyhydroxide minerals in weathering environments (Kabata-Pendias and Mukherjee, 2007). Germanium has a particular affinity for organic material, which may be one of the mechanisms of germanium enrichment in coal.

The tendency for germanium and indium to be dissolved and transported largely depends upon the pH and temperature of weathering solutions. Both elements are commonly concentrated in sulfide minerals and are therefore relatively mobile under most weathering conditions because of the instability of sulfide minerals subjected to near-surface oxidizing conditions. Oxidative dissolution of sulfide minerals releases metals and sulfuric acid, resulting in the environmental problem known as acid mine drainage (AMD). Metals, including germanium and indium, dissolved in acidic drainage can be attenuated through precipitation, sorption to (oxyhydr)oxide minerals, or dilution by mixing with water at circum-neutral pH; otherwise, metals are transported downstream.

Examples of natural concentrations of germanium in soil and water are given in table I3. Germanium contents in soils generally range from 0.5 to 2.3 ppm (Shacklette and Boerngen, 1984; Eriksson, 2001), and concentrations as high as 173 ppm have been observed in soil in Sweden (Eriksson, 2001). Germanium concentrations in seawater range from nearly 0.05 to 13 parts per trillion (ppt) (Froelich and others, 1985; Santosa and others, 1997; Ellwood and Maher, 2003); seawater germanium concentrations follow a typical nutrient profile, as the surface water is more depleted of germanium than the bottom water (Froelich and others, 1985). Seawater germanium concentrations are generally lower than the 2 to 80 ppt range (mean is 7 ppt) observed for uncontaminated rivers around the world (Froelich and others, 1985; Mortlock and Froelich, 1987; Gaillardet and others, 2003). Geothermal waters contain higher germanium contents, as evidenced by the range observed in hot springs (1,500 to 6,800 ppt) in the Cascade Range, United States (Siebert and others, 2006). Compared to dissolved forms, germanium is highly concentrated in small particulates in river water; the global average in suspended sediment is 1,230,000 ppt (1.23 ppm) (Viers and others, 2009).

Examples of natural concentrations of indium in soil, water, and air are given in table I4. The general worldwide indium content in soils ranges from 0.01 to 0.5 ppm (Kabata-Pendias and Pendias, 2001). Indium concentrations in soils in the United States range from less than 0.02 to 0.12 ppm (Smith and others, 2005), and in soils in Sweden, from less than 0.04 to 0.07 ppm (Eriksson, 2001). Indium concentrations in seawater generally range from 0.003 to 1.23 ppt (Amakawa and others, 1996; Alibo and others, 1999; Nozaki, Lerche, Alibo, and Snidvongs, 2000; Obata and others, 2007), although dissolved and particulate indium in seawater near Japan has been measured to be as high as 4.7 and 35 ppt, respectively (Miyazaki and others, 2012). Rivers and lakes in Japan contain dissolved indium in concentrations ranging from 0.16 to 3.2 ppt (Nozaki, Lerche, Alibo, and Tsutsumi, 2000; Miyazaki and others, 2012), whereas indium in particulate matter in rivers in Japan can be as high as 12.8 ppt (Miyazaki and others, 2012). Indium occurs naturally in the atmosphere as part of mineral dust particles; indium concentrations of 0.05 and 20 picograms per cubic meter (pg/m^3) of air have been measured in remote regions (Kabata-Pendias and Pendias, 2001, and references therein).

Above-background concentrations of germanium and indium in the environment can result from mining and ore processing, particularly of zinc, lead, and sometimes copper sulfide ores. Total emissions of indium to the atmosphere from copper and zinc production were estimated to be between 11,000 and 39,000 kilograms per year during 1983 (Nriagu and Pacyna, 1988). Air indium concentrations over more-industrialized regions may range from 20 to 1,200 pg/m^3 (Kabata-Pendias and Pendias, 2001, and references therein). Likewise, the concentration of indium in air near a lead-smelting complex was measured as 5,800 pg/m^3 (Ragaini and others, 1977). In addition to mining and ore processing inputs, anthropogenic release of germanium to the atmosphere occurs during coal combustion. For example, dissolved median germanium concentrations in world rivers are 7 ppt in locations distant from and 24 ppt in locations proximal to coal combustion centers, respectively (Froelich and others, 1985).

The recycled content, or proportion of scrap, used in germanium and indium production is between 25 and 50 percent, and the fraction of germanium and indium in discarded products that get recycled is less than 1 percent (Graedel and others, 2011). One of the main challenges of germanium and indium recycling is that these metals are often comingled with other “specialty metals” in high performance alloys, making recovery technologically and economically unfeasible (Reck and Graedel, 2012). Given the importance of germanium and indium in emerging technologies, however, germanium and indium recycling is likely to increase in the future.

Table I3. Germanium concentrations in rocks, soils, and waters.

[cm, centimeter; ppm, part per million; ppt, part per trillion; µm, micrometer]

Environment and (or) location	Germanium concentration	Unit	Notes	Reference(s)
			Rocks	
Upper continental crust	1.6	ppm	Average	Taylor and McLennan (1995)
Bulk continental crust	1.6	ppm	Average	Taylor and McLennan (1995)
Lower continental crust	1.6	ppm	Average	Taylor and McLennan (1995)
			Soils	
Western United States	1.2	ppm	Mean for 20 cm depth	Shacklette and Boerngen (1984)
Eastern United States	1.1	ppm	Mean for 20 cm depth	Shacklette and Boerngen (1984)
Topsoil, Sweden	<1.0 to 95	ppm	Range; median is 7 ppm	Eriksson (2001)
Subsoil, Sweden	<1.0 to 173	ppm	Range; median is 21 ppm	Eriksson (2001)
			Waters	
Antarctic Ocean	0.4 to 7.3	ppt	Unfiltered; profile with enriched bottom water	Froelich and others (1985)
North Atlantic Ocean	<0.4 to 2.9	ppt	Unfiltered; profile with enriched bottom water	Froelich and others (1985)
Pacific Ocean	<0.07 to 2.5	ppt	Range of averages for surface water; dissolved and colloidal (<0.45 µm)	Santosa and others (1997)
Pacific Ocean (northwestern)	0.4 to 8.7	ppt	Unfiltered; profile with enriched bottom water	Froelich and others (1985)
South Pacific Ocean (New Zealand)	0.05 to 0.28	ppt	Dissolved (<0.2 µm); surface water	Ellwood and Maher (2003)
South Pacific Ocean (New Zealand)	0.09 to 1.9	ppt	Dissolved (<0.2 µm); profile with enriched bottom water	Ellwood and Maher (2003)
Bering Sea	1.8 to 13	ppt	Unfiltered; profile with enriched bottom water	Froelich and others (1985)
World rivers	2 to 18	ppt	Dissolved and colloidal (<0.4 µm); median is 7 ppt distant from coal combustion areas	Froelich and others (1985)
World rivers—Contaminated (near coal combustion or Ge refinery areas)	0.7 to 3,050	ppt	Dissolved and colloidal (<0.4 µm); median is 24 ppt near heavy coal combustion areas	Froelich and others (1985)
Small rivers worldwide	2 to 20	ppt	Dissolved and colloidal (<0.4 µm)	Mortlock and Froelich (1987)
African rivers	6.5 to 80	ppt	Dissolved load (<0.2 µm)	Gaillardet and others (2003)
North American rivers	1.4 to 22	ppt	Dissolved load (<0.2 µm)	Gaillardet and others (2003)
South American rivers	4 to 8	ppt	Dissolved load (<0.2 µm)	References within Gaillardet and others (2003)
Amazon River, South America	5 to 11	ppt	Dissolved and colloidal (<0.4 µm)	Mortlock and Froelich (1987)
Changjiang River, China	12.2	ppt	Dissolved load (<0.2 µm)	Gaillardet and others (2003)
Columbia River, United States	12 to 20	ppt	Dissolved and colloidal (<0.4 µm)	Mortlock and Froelich (1987)
Congo River, Africa	6 to 9	ppt	Dissolved and colloidal (<0.4 µm)	Mortlock and Froelich (1987)
Idle River, England	8.2	ppt	Dissolved load (<0.2 µm)	References within Gaillardet and others (2003)
Yukon River, North America	4 to 5	ppt	Dissolved and colloidal (<0.4 µm)	Mortlock and Froelich (1987)
World rivers—Sediment	1,230,000	ppt	1.23 ppm; average suspended sediment	Viers and others (2009)
Hotsprings, Cascades, United States	1,500 to 6,800	ppt	Samples described in references	Siebert and others (2006) and references therein
Geothermal waters	<24 to 293	ppb	None	Höll and others (2007)

Table I4. Indium concentrations in rocks, soils, waters, and air.

[b.d.l., below detection limit; cm, centimeter; µm, micrometer: ppm, part per million; ppt, part per trillion; pg/m^3, picogram per cubic meter]

Environment and (or) location	Indium concentration	Unit	Notes	Reference(s)
			Rocks	
Upper continental crust	0.05	ppm	Average	Taylor and McLennan (1995)
Bulk continental crust	0.05	ppm	Average	Taylor and McLennan (1995)
Lower continental crust	0.05	ppm	Average	Taylor and McLennan (1995)
			Soils	
Soils, worldwide	0.01 to 0.5	ppm	None	Kabata-Pendias and Pendias (2001)
Conterminous United States	<0.02 to 0.12	ppm	0 to 5 cm depth; median is 0.04 ppm	Smith and others (2005)
Conterminous United States	<0.02 to 0.04	ppm	O horizon, if present; median is 0.03 ppm	Smith and others (2005)
Conterminous United States	<0.02 to 0.12	ppm	A horizon; median is 0.04 ppm	Smith and others (2005)
Conterminous United States	<0.02 to 0.10	ppm	C horizon; median is 0.04 ppm	Smith and others (2005)
Topsoil, Sweden	<0.04 to 0.064	ppm	Median is <0.04 ppm	Eriksson (2001)
Subsoil, Sweden	<0.04 to 0.073	ppm	Median is 0.02 ppm	Eriksson (2001)
			Waters	
Seawater, North Atlantic Ocean	0.07 to 0.19	ppt	Dissolved and colloidal (<0.45 µm)	Alibo and others (1999)
Seawater, northwest Pacific Ocean	0.005 to 0.018	ppt	Unfiltered	Amakawa and others (1996)
Seawater, Mediterranean	0.72 to 1.23	ppt	Dissolved and colloidal (<0.6 µm)	Alibo and others (1999)
Seawater, Japan	b.d.l. to 4.7	ppt	Particulate; median is 3.1 ppt	Miyazaki and others (2012)
Seawater, Japan	0.2 to 34.8	ppt	Dissolved and colloidal (<0.45 µm); median is 2.6 ppt	Miyazaki and others (2012)
Sea of Japan	0.005 to 0.067	ppt	Dissolved (<0.04 µm)	Obata and others (2007)
River water, Japan	0.16 to 1.7	ppt	Dissolved (<0.04 µm)	Nozaki, Lerche, Alibo, and Tsutsumi (2000)
River water, Japan	b.d.l. to 3.2	ppt	Dissolved and colloidal (<0.45 µm)	Miyazaki and others (2012)
River water, Japan	b.d.l. to 12.8	ppt	Particulate	Miyazaki and others (2012)
Lake water, Japan	1.1 to 3.2	ppt	Dissolved and colloidal (<0.45 µm)	Miyazaki and others (2012)
Lake water, Japan	1.5 to 3.2	ppt	Particulate	Miyazaki and others (2012)
Estuary, Thailand	0.003 to 0.049	ppt	Dissolved (<0.04 µm)	Nozaki, Lerche, Alibo, and Snidvongs (2000)
			Air	
North America	20 to 140	pg/m^3	None	Kabata-Pendias and Pendias (2001) and references therein
South Pole	0.05	pg/m^3	None	Kabata-Pendias and Pendias (2001) and references therein
Idaho, United States	5,800	pg/m^3	Near a lead smelter complex	Ragaini and others (1977)
Japan	1,200	pg/m^3	None	Kabata-Pendias and Pendias (2001) and references therein
Shetland Islands	20	pg/m^3	None	Kabata-Pendias and Pendias (2001) and references therein
West Germany	30 to 360	pg/m^3	None	Kabata-Pendias and Pendias (2001) and references therein

Mine Waste Characteristics

Mine waste is generally considered to be the material that originates and accumulates at a mine site that has no current economic value (Lottermoser, 2010); it includes both solid and liquid waste. Mine waste that results from extraction of germanium- and indium-bearing copper-lead-zinc ore usually consists of waste rock and tailings piles, and possibly pit lakes. Tailings are the residual silt- to fine-sand-sized grains that result from ore grinding and processing, and they are usually disposed of in waste dumps. Germanium is often recovered from ores in SEDEX zinc-lead-silver deposits, such as at the Red Dog Mine in Alaska, and from MVT lead-zinc deposits, such as those in the Tri-State mining district, which covers approximately 1,800 square kilometers of Kansas, Oklahoma, and Missouri (Butterman and Jorgenson, 2005). Indium can be concentrated in ores in vein stockwork tin and tungsten deposits, such as the Mount Pleasant Mine in New Brunswick, Canada, and in VMS deposits, such as the Kidd Creek Mine in Ontario, Canada (Jorgenson and George, 2004). The tonnage of tailings generated at the Red Dog Mine totaled 27.4 million metric tons in 2006 and is projected to total 88 million metric tons by 2031 (SRK Consulting (Canada) Inc., 2007). The Tri-State mining district is the largest U.S. Environmental Protection Agency Superfund site in the United States (Leach and others, 2010); the estimated total tonnage of waste rock at this site is 91 million metric tons (U.S. Environmental Protection Agency, 2006). In 1999, the Kidd Creek mining and metallurgical operation stored more than 100 million metric tons of tailings over an area of approximately 1,200 hectares (Al and Blowes, 1999).

The mineralogy of the mine waste in germanium- and indium-enriched deposits tends to be similar to the mineralogy of the deposit, except that the proportion of sulfides, such as sphalerite, galena (PbS), and chalcopyrite ($CuFeS_2$), is reduced relative to typical gangue minerals, such as barite ($BaSO_4$), calcite ($CaCO_3$), dolomite ($(Ca,Mg)(CO_3)_2$), pyrite (FeS_2), pyrrhotite ($Fe_{1-x}S$), and quartz (SiO_2) (Kelley and others, 1995; Leach and others, 1995; Taylor and others, 1995). For example, tailings from the Kidd Creek deposit contain (in weight percent) quartz and various silicates (75 to 85), pyrite (10 to 25), carbonate minerals (7 to 8) pyrrhotite (1 to 2), and sphalerite and chalcopyrite (1 to 2) (Al and others, 1994). Indium-enriched VMS deposits may also contain anhydrite ($CaSO_4$) and gypsum ($CaSO_4 \cdot 2H_2O$), chlorite ($(Mg,Fe)_3(Si,Al)_4O_{10}(OH)_2(Mg,Fe)_3(OH)_6$, and magnetite ($Fe_3O_4$) as gangue minerals (Taylor and others, 1995). Some deposits undergo appreciable weathering before discovery, which can result in oxidized zones on the surface of orebodies known as gossan. Minerals that precipitate from the weathering of ore minerals in gossan commonly include amorphous silica (SiO_2), goethite (FeO(OH)), jarosite ($KFe^{III}_3(OH)_6(SO_4)_2$) and other hydroxysulfate minerals, scorodite ($FeAsO_4 \cdot 2H_2O$), and secondary sulfide minerals, such as chalcocite (Cu_2S) and covellite (CuS) (Taylor and others, 1995).

Because of their association with sulfide and secondary minerals, elements such as Ag, Al, As, Au, B, Ba, Bi, Cd, Co, Cu, F, Fe, Ga, Hg, Mn, Mo, Ni, Pb, Sb, Sn, and Zn can be found in germanium- and indium-enriched mineral deposits (Briskey, 1986; Kelley and others, 1995; Leach and others, 1995; Taylor and others, 1995). During oxidizing and acidic ($pH < 3$) weathering conditions, which may be expected in mine waste with little to no acid-neutralizing capacity, many of these accessory elements are expected to be mobile (Smith and Huyck, 1999). The acid-neutralizing capacity of carbonate-hosted MVT mine waste is expected to be greater, however, resulting in the accessory elements listed above being less mobile or immobile under oxidizing and circum-neutral ($5 < pH < 8$) weathering conditions (Smith and Huyck, 1999). The exception is zinc, which can make up a large percentage of total dissolved metals draining from MVT deposits (Plumlee and others, 1999).

Human Health Concerns

Both germanium and indium have no known physiological role in human biochemical functions, and thus are considered to be nonessential. Germanium and indium can be ingested through food and inhaled with dust in industrial environments. For example, workers in an indium ingot manufacturing plant who were exposed to insoluble indium compounds through inhalation showed higher concentrations of indium in plasma and urine relative to a control group (Hoet and others, 2012). Germanium toxicity is generally low, and germanium does not appear to be carcinogenic; to the contrary, the organic germanium compound spirogermanium has been shown to destroy cancer cells (Gerber and Léonard, 1997, and references therein). Excessive ingestion of germanium has taken place owing to the belief that germanium in supplements has antioxidant properties. This has led to renal failure and renal and multiorgan dysfunction (Glei, 2004, and references therein). Unlike solid germanium compounds, the gas germane (GeH_4) is highly toxic and can be lethal at concentrations near 150 ppm or higher (Glei, 2004, and references therein). As a result, the U.S. Occupational Safety and Health Administration (OSHA) has set a permissible exposure limit of 0.2 ppm GeH_4 over an 8-hour workday (Occupational Safety and Health Administration, 2013a).

The human toxicity of indium is relatively well documented, partly because the short half-life of radioactive ^{111}In lends itself to use in nuclear medicine to study inflammatory processes and tumors (Madden and others, 2004, and references therein). Industrial workers may be exposed to insoluble indium compounds, such as indium arsenide, indium phosphide, and ITO, all of which have proven to be toxic to animals. Chronic (low doses over extended time periods) exposure to inhaled indium phosphide, in particular, has shown carcinogenic effects in animals (Tanaka and others, 2010). A few case studies of workers exposed to insoluble indium compounds have shown that inhaled indium can cause interstitial lung damage (Hamaguchi and others, 2008, and

references therein). Furthermore, among the metal arsenic compounds used in the semiconductor industry, indium arsenide has proven to cause the greatest impairment to lung function (Tanaka, 2004, and references therein). To prevent negative effects from occupational indium exposure, OSHA has set a limit of 0.1 milligram per cubic meter for indium-bearing dust in workplace air over an 8-hour workday (Occupational Safety and Health Administration, 2013b).

Mining of zinc-lead-copper deposits, where germanium and indium may be byproducts, can potentially mobilize elements that are known human toxins. Lead and arsenic are perhaps the best-known examples of chemicals that are released into the environment through mining and that end up in drinking water. Lead is known to affect the neurological development of children (Holecy and Mousavi, 2012), and arsenic is known to have carcinogenic effects (Gupta and others, 2012). Other associated elements also have the potential to affect human health when present above threshold concentrations in air, drinking water, and soil. The current U.S. National Ambient Air Quality Standard for lead is 0.15 micrograms per cubic meter (U.S. Environmental Protection Agency, 2013b), and the current U.S. primary and secondary drinking water standards for lead, copper, and zinc are 0, 1, and 5 milligrams per liter (mg/L), respectively (U.S. Environmental Protection Agency, 2013a). Canadian agricultural soil quality guidelines for copper, lead, and zinc are 63, 70, and 200 ppm, respectively (Canadian Council of Ministers of the Environment, 1999). These concentrations are sometimes exceeded near mine sites and ore processing plants.

Ecological Health Concerns

Relatively few studies have focused on the ecological impacts of germanium and indium mobility in the environment. One of several useful endpoints used in toxicity tests is the lethal concentration that leads to 50 percent mortality (LC_{50}) after exposure to a substance for a certain amount of time. Fish tend to be sensitive to low concentrations of dissolved metals, and they are therefore useful indicators of contamination in aquatic systems. Chronic toxicity tests with dissolved germanium (in the form of GeO_2) and developing rainbow trout (*Oncorhynchus mykiss*) revealed a mean LC_{50} value of 0.05 mg/L after 28 days of exposure (Birge and others, 1980). Another aquatic organism that is commonly used in toxicity studies is the freshwater amphipod *Hyalella azteca*. The 1-week LC_{50} for germanium incubated with *H. azteca* was 0.21 ppm in soft water and more than 3.15 ppm in hard water (Borgmann and others, 2005). An *in vitro* study of the effects of indium nitrate ($In(NO_3)_3$) on fish cells revealed that cell proliferation was significantly reduced at indium concentrations of 356 ppm (3-day exposure) and 677 ppm (1-day exposure) (Zurita and others, 2007). Exposure of indium nitrate to the bacterium *Aliivibrio fischeri*, the alga *Chlorella vulgaris*, and the cladoceran *Daphnia magna* resulted in 50 percent of populations exhibiting decreased functionality over a range of effective concentrations (EC_{50}), with the most sensitive EC_{50} being inhibited bioluminescence of *A. fischeri* at 6 ppm indium (Zurita and others, 2007). These indium concentrations are orders of magnitude greater than those in reported natural systems (table I4). Germanium and indium are usually not included in the suite of elements in studies of the chemistry of mine waste water, however, so the toxicity endpoint concentrations cannot be compared to likely germanium and indium concentrations in mining environments.

Plant tissues contain from 50 to 754 ppm germanium and 1 to 2 ppm indium (Kabata-Pendias and Mukherjee, 2007), although neither element is known to have any physiological function in plants. In a study of barley seedlings exposed to nutrient solutions with varying germanium concentrations, roots and shoots accumulated greater amounts of germanium with increasing germanium concentrations, and the only toxic effects observed were necrosis of primary leaves at concentrations greater than 1.45 ppm germanium (Halperin and others, 1995). The effects of indium on plants remain unknown.

The ecological impacts of major metals with which germanium and indium are associated are relatively well documented. For example, in toxicity tests with aquatic invertebrates incubated with lead-zinc mine tailings from the Tri-State mining district, Besser and Rabeni (1987) showed that increased concentrations of dissolved cadmium, lead, and zinc correlated with decreased survival and growth (Besser and Rabeni, 1987). Likewise, various fish species experienced rapid mortality when exposed to increasing dissolved zinc concentrations, but this effect decreased with increasing calcium, magnesium, and sodium concentrations (De Schamphelaere and Janssen, 2004). High metal concentrations in soils can also cause phytotoxicity. Zinc is a micronutrient for many plant species, but, when highly concentrated in soils, it can inhibit a plant's metabolic functions and cause deficiencies in other essential nutrients, such as copper, iron, manganese, and phosphorus (Nagajyoti and others, 2010, and references therein).

Carbon Footprint

Indium is used in some of the most efficient thin-film photovoltaic cells (solar panels) (Miles and others, 2007) and has potential to help reduce the carbon dioxide (CO_2) emissions from energy production. The copper-indium–gallium-diselenide (CIGS) alloy, among others, is becoming an increasingly preferred thin-film product because of its relatively low material and manufacturing costs (Kaneshiro and others, 2010). The CIGS photovoltaic cells are in the initial stages of commercialization, but they are expected eventually to compete with other forms of energy production as economies of scale permit future cost reductions (Miles and others, 2007; Rockett, 2010). The recyclability of generated products and the potential for leaching of toxic elements from improperly disposed of industrial products are subjects that no doubt will need to be addressed as the use of thin-film photovoltaic cells increases.

Mine Closure

Most recent and new mining operations include closure plans that address issues related to the mine footprint. A mine's footprint includes the waste left on site and locally impacted soil and water, as well as ecological impacts, such as habitat destruction and loss of biodiversity. Following mining in copper-lead-zinc deposits, where germanium and indium may be byproducts, a common mine closure issue is the potential for AMD from the site. Acidic drainage may seep from waste piles or tailings ponds, and common remediation methods include active water treatment facilities, passive limestone-lined channels, or constructed wetlands (Plumlee and Logsdon, 1999). The end result of both active and passive approaches is eventual precipitation of dissolved metals. Precipitated metals tend to be more stable under the prevailing anoxic conditions in passive wetland systems, whereas the metal-rich precipitates that result from active treatment facilities form a sludge that can cause environmental problems if not responsibly treated.

At large mines, mine waste is often consolidated into pits and submerged under water, forming a tailings pond or impoundment. Acid-generating minerals typically are less reactive under water because of limited oxygen, but any seepage usually needs to be treated. At sites like the Red Dog Mine, seepage from the tailings pond will need to be treated in perpetuity (U.S. Environmental Protection Agency, 2010). The massive tailings impoundment near the Kidd Creek Mine is designed to have a conical shape. This limits the amount of tailings that may oxidize in near-surface unsaturated zones and contribute soluble metals, which allows more control over the AMD effluent discharged at the periphery of the impoundment (Al and Blowes, 1999). When the potential for AMD exists at a mine site, a common mine closure plan includes conducting water-quality surveys before, during, and after mining.

Another common mine closure issue related to mining in germanium- and indium-enriched deposits is the creation of large, dry mounds of mine-waste. These waste piles have the potential to become unstable and can be a source of metal-rich dust. If using mine waste as backfill into mine workings is not an option, mine waste pile stability and dust-generating issues can often be addressed through grading and covering piles with vegetation. Securing waste piles and prevention and treatment of AMD are typically figured into the long-term costs of active and proposed metal mining projects.

Problems and Future Research

Weeks (1973) and Brobst and Pratt (1973) pointed out that resource studies of minor byproduct metals are limited by inadequate data, and that is still true today. The sources of the materials that are processed at smelters for byproduct germanium and indium are often either not carefully tracked or the information is considered proprietary. Data on the distribution of germanium and indium are improving but currently are still not sufficient to understand content variations in different deposits and especially in different zones in given deposits. Additional systematic analytical data are needed to establish the overall grades of germanium and indium in different deposits, and the potentially economic resources that might be available in such deposits. The most promising areas of research involve studies of the distribution of germanium and indium in copper and zinc ore deposits and coal deposits, and the making of a systematic compilation of local and regional variations.

Significant concentrations of these elements are not currently recovered in the processing of other ores, particularly zinc and (or) copper ores; the addition of more recovery facilities and improvement in metallurgical techniques could significantly increase supplies. Finally, recycling of germanium and indium from electronic products and from manufacturing waste is presently a significant contributor to the production of these mineral commodities, and improving the recycling processes could help increase supplies significantly (Bleiwas, 2010).

References Cited

Note: All Web links listed were active as of the access date but may no longer be available.

Al, T.A., and Blowes, D.W., 1999, The hydrogeology of a tailings impoundment formed by central discharge of thickened tailings—Implications for tailings management: Journal of Contaminant Hydrology, v. 38, no. 4, p. 489–505. [Also available at http://dx.doi.org/10.1016/s0169-7722(99)00007-8.]

Al, T.A., Blowes, D.W., Jambor, J.L., and Scott, J.D., 1994, The geochemistry of mine-waste pore water affected by the combined disposal of natrojarosite and base-metal sulphide tailings at Kidd Creek, Timmins, Ontario: Canadian Geotechnical Journal, v. 31, no. 4, p. 502–512. [Also available at http://dx.doi.org/10.1139/t94-059.]

Alfantazi, A.M., and Moskalyk, R.R., 2003, Processing of indium—A review: Minerals Engineering, v. 16, no. 8, p. 687–694. [Also available at http://dx.doi.org/10.1016/s0892-6875(03)00168-7.]

Alibo, D.S., Nozaki, Yoshiyuki, and Jeandel, Catherine, 1999, Indium and yttrium in North Atlantic and Mediterranean waters—Comparison to the Pacific data: Geochimica et Cosmochimica Acta, v. 63, nos. 13–14, p. 1991–1999. [Also available at http://dx.doi.org/10.1016/s0016-7037(99)00080-0.]

Amakawa, Hiroshi, Alibo, D.S., and Nozaki, Yoshiyuki, 1996, Indium concentration in Pacific seawater: Geophysical Research Letters, v. 23, no. 18, p. 2473–2476. [Also available at http://dx.doi.org/10.1029/96gl02300.]

Bernstein, L.R., 1986, Geology and mineralogy of the Apex germanium-gallium mine, Washington County, Utah: U.S. Geological Survey Bulletin 1577, 9 p. [Also available at http://pubs.er.usgs.gov/publication/b1577.]

Besser, J.M., and Rabeni, C.F., 1987, Bioavailability and toxicity of metals leached from lead-mine tailings to aquatic invertebrates: Environmental Toxicology and Chemistry, v. 6, no. 11, p. 879–890. [Also available at http://dx.doi.org/10.1002/etc.5620061109.]

Birge, W.J., Black, J.A., Westerman, A.G., and Hudson, J.E., 1980, Aquatic toxicity tests on inorganic elements occurring in oil shale, *in* Gale, Charles, ed., Oil shale symposium—Sampling, analysis, and quality assurance, March 1979, Proceedings: Cincinnati, Ohio, U.S. Environmental Protection Agency, EPA-600/9–80–022, p. 519–534. [Also available at http://babel.hathitrust.org/cgi/pt?id=coo.31924004323303;view=1up;seq=531.]

Bischoff, J.L., Rosenbauer, R.J., Arascavage, P.J., Baedecker, P.A., and Crock, J.G., 1983, Sea-floor massive sulfide deposits from 21° N, East Pacific Rise; Juan de Fuca Ridge; and Galapagos Rift—Bulk chemical composition and economic implications: Economic Geology, v. 78, p. 1711–1720. [Also available at http://dx.doi.org/10.2113/gsecongeo.78.8.1711.]

Bleiwas, D.I., 2010, Byproduct mineral commodities used for the production of photovoltaic cells: U.S. Geological Survey Circular 1365, 10 p., accessed November 30, 2015, at http://pubs.er.usgs.gov/publication/cir1365.

Borgmann, Uwe, Couillard, Yves, Doyle, Patrick, and Dixon, D.G., 2005, Toxicity of sixty-three metals and metalloids to *Hyalella azteca* at two levels of water hardness: Environmental Toxicology and Chemistry, v. 24, no. 3, p. 641–652. [Also available at http://dx.doi.org/10.1897/04-177r.1.]

Briskey, J.A., 1986, Descriptive model of sedimentary exhalative Zn-Pb—Model 31a, *in* Cox, D.P., and Singer, D.A., eds., Mineral deposit models: U.S. Geological Survey Bulletin 1693, p. 211–212. [Also available at http://pubs.er.usgs.gov/publication/b1693.]

Brobst, D.A., and Pratt, W P., eds., 1973, United States mineral resources: U.S. Geological Survey Professional Paper 820, 722 p., accessed November 30, 2015, at http://pubs.er.usgs.gov/publication/pp820.

Burgin, L.B., 1988, The mineral industry of Utah, *in* Area reports—Domestic: U.S. Bureau of Mines Minerals Yearbook 1986, v. II, p. 475–490.

BusinessWire, 2013, Amonix achieves world record 35.9% PV module efficiency rating at NREL: BusinessWire, August 20, accessed April 14, 2016, at http://www.businesswire.com/news/home/20130820005361/en/Amonix-Achieves-World-Record-35.9-PV%C2%A0Module-Efficiency.

Butterman, W.C., and Jorgenson, J.D., 2005, Mineral commodity profiles—Germanium: U.S. Geological Survey Open-File Report 2004–1218, 19 p., accessed November 30, 2015, at http://pubs.er.usgs.gov/publication/ofr20041218.

Canadian Council of Ministers of the Environment, 1999, Canadian soil quality guidelines for the protection of environmental and human health, in Canadian environmental quality guidelines, chap. 7 *of* Canadian environmental quality guidelines: Winnipeg, Manitoba, Canada, Canadian Council of Ministers of the Environment, accessed February 15, 2013, at http://ceqg-rcqe.ccme.ca/en/index.html.

Chaplygin, I.V., Mozgova, N.N., Mokhov, A.V., Koporulina, E.V., Bernhardt, H.-J., and Bryzgalov, I.A., 2007, Minerals of the system ZnS-CdS from fumaroles of the Kudriavy volcano, Iturup Island, Kuriles, Russia: The Canadian Mineralogist, v. 45, no. 4, p. 709–722. [Also available at http://dx.doi.org/10.2113/gscanmin.45.4.709.]

Cox, D.P., and Singer, D.A., eds., 1986, Mineral deposit models: U.S. Geological Survey Bulletin 1693, 379 p. [Also available at http://pubs.er.usgs.gov/publication/b1693.]

De Schamphelaere, K.A.C., and Janssen, C.R., 2004, Bioavailability and chronic toxicity of zinc to juvenile rainbow trout (*Oncorhynchus mykiss*)—Comparison with other fish species and development of a biotic ligand model: Environmental Science and Technology, v. 38, no. 23, p. 6201–6209. [Also available at http://dx.doi.org/10.1021/es049720m.]

De Vera, J., McClay, K.R., and King, A.R., 2004, Structure of the Red Dog district, western Brooks Range, Alaska: Economic Geology, v. 99, p. 1415–1434.

Ellwood, M.J., and Maher, W.A., 2003, Germanium cycling in the waters across a frontal zone—The Chatham Rise, New Zealand: Marine Chemistry, v. 80, nos. 2–3, p. 145–159. [Also available at http://dx.doi.org/10.1016/s0304-4203(02)00115-9.]

Eriksson, Jan, 2001, Concentrations of 61 trace elements in sewage sludge, farmyard manure, mineral fertilizer, precipitation and in oil and crops: Swedish Environmental Protection Agency Report 5159, 69 p. [Also available at http://www.naturvardsverket.se/Documents/publikationer/620-6246-8.pdf.]

European Commission, 2010, Report forecasts shortages of 14 critical mineral raw materials: European Commission press release IP–10–752, June 17, 3 p., accessed March 2, 2016, at http://europa.eu/rapid/press-release_IP-10-752_en.htm. [Additional information accessed April 7, 2016, at http://ec.europa.eu/growth/sectors/raw-materials/specific-interest/critical/index_en.htm.]

Froelich, P.N., Blanc, V., Mortlock, R.A., Chillrud, S.N., Dunstan, W., Udomkit, A., and Peng, T.-H., 1992, River fluxes of dissolved silica to the ocean were higher during glacials—Ge/Si in diatoms, rivers, and oceans: Paleoceanography, v. 7, no. 6, p. 739–767. [Also available at http://dx.doi.org/10.1029/92pa02090.]

Froelich, P.N., Hambrick, G.A., Andreae, M.O., Mortlock, R.A., and Edmond, J.M., 1985, The geochemistry of inorganic germanium in natural waters: Journal of Geophysical Research—Oceans, v. 90, no. C1, p. 1133–1141. [Also available at http://dx.doi.org/10.1029/jc090ic01p01133.]

Gaillardet, J., Viers, J., and Dupré, B., 2003, Trace elements in river waters, *in* Drever, J.I., ed., Surface and ground water, weathering, and soils, v. 5 *of* Holland, H.D., and Turekian, K.K., eds., Treatise on geochemistry: Oxford, United Kingdom, Elsevier-Pergamon, p. 225–272. [Also available at http://dx.doi.org/10.1016/B0-08-043751-6/05165-3.]

Gerber, G.B., and Léonard, A., 1997, Mutagenicity, carcinogenicity and teratogenicity of germanium compounds: Mutation Research, v. 387, no. 3, p. 141–146. [Also available at http://dx.doi.org/10.1016/s1383-5742(97)00034-3.]

Glei, Michael, 2004, Germanium, chap. 10 *of* Merian, Ernest, Anke, Manfred, Ihnat, Milan, and Stoeppler, M.S, eds., Elements and their compounds in the environment—Occurrence, analysis and biological relevance: Weinheim, Germany, Wiley-VCH Verlag GmbH, pt. 3, p. 787–793. [Also available at http://dx.doi.org/10.1002/9783527619634.ch31.]

Goodfellow, W.D., and Lydon, J.W., 2007, Sedimentary exhalative (SEDEX) deposits, *in* Goodfellow, W.D., ed., Mineral deposits of Canada—A synthesis of major deposit-types, district metallogeny, the evolution of geological provinces, and exploration methods: Geological Association of Canada, Special Publication no. 5, p. 163–184.

Graedel, T.E., Allwood, Julian, Birat, J.-P., Buchert, Matthias, Hagelüken, Christian, Reck, B.K., Sibley, S.F., and Sonnemann, Guido, 2011, What do we know about metal recycling rates?: Journal of Industrial Ecology, v. 15, no. 3, p. 355–365. [Also available at http://dx.doi.org/10.1111/j.1530-9290.2011.00342.x.]

Guberman, D.E., 2013a, Germanium: U.S. Geological Survey Mineral Commodity Summaries 2013, p. 64–65, accessed November 30, 2015, at http://minerals.usgs.gov/minerals/pubs/commodity/germanium/mcs-2013-germa.pdf.

Guberman, D.E., 2013b, Germanium (Ge), *in* Metal prices in the United States through 2010: U.S. Geological Survey Scientific Investigations Report 2012–5188, p. 55–57, accessed May 24, 2016, at http://pubs.usgs.gov/sir/2012/5188/.

Guberman, D.E., 2014, Germanium: U.S. Geological Survey Mineral Commodity Summaries 2014, p. 64–65, accessed September 12, 2016, at https://minerals.usgs.gov/minerals/pubs/commodity/germanium/mcs-2014-germa.pdf.

Gu, Lianxing, Zaw, Khin, Hu, Wenxuan, Zhang, Kaijun, Ni, Pei, He, Jinxiang, Xu, Yaotong, Lu, Jianjun, and Lin, Chunming, 2007, Distinctive features of Late Palaeozoic massive sulphide deposits in South China: Ore Geology Reviews, v. 31, p. 107–138. [Also available at http://dx.doi.org/10.1016/j.oregeorev.2005.01.002.]

Gupta, V.K., Nayak, Arunima, Agarwal, Shilpi, Dobhal, Rajendra, Uniyal, D.P., Singh, Prashant, Sharma, Bhavtosh, Tyagi, Shweta, and Singh, Rakesha, 2012, Arsenic speciation analysis and remediation techniques in drinking water: Desalination and Water Treatment, v. 40, nos. 1–3, p. 231–243, [Also available at http://dx.doi.org/10.1080/19443994.2012.671250.]

Halperin, S.J., Barzilay, Adam, Carson, Matthew, Roberts, Cory, and Lynch, Jonathan, 1995, Germanium accumulation and toxicity in barley: Journal of Plant Nutrition, v. 18, no. 7, p. 1417–1426. [Also available at http://dx.doi.org/10.1080/01904169509364991.]

Hamaguchi, T., Omae, K., Takebayashi, T., Kikuchi, Y., Yoshioka, N., Nishiwaki, Y., Tanaka, A., Hirata, M., Taguchi, O., and Chonan, T., 2008, Exposure to hardly soluble indium compounds in ITO production and recycling plants is a new risk for interstitial lung damage: Occupational and Environmental Medicine, v. 65, no. 1, p. 51–55. [Also available at http://dx.doi.org/10.1136/oem.2006.029124.]

Hoet, Perrine, De Graef, Emmy, Swennen, Bert, Seminck, Théo, Yakoub, Yousof, Deumer, Gladys, Haufroid, Vincent, and Lison, Dominique, 2012, Occupational exposure to indium—What does biomonitoring tell us?: Toxicology Letters, v. 213, no. 1, p. 122–128. [Also available at http://dx.doi.org/10.1016/j.toxlet.2011.07.004.]

Holecy, E.G., and Mousavi, Aliyar, 2012, Lead sources, toxicity, and human risk in children of developing countries—A mini-review: Environmental Forensics, v. 13, no. 4, p. 289–292. [Also available at http://dx.doi.org/10.1080/15275922.2012.729010.]

Höll, R., Kling, M., and Schroll, E., 2007, Metallogenesis of germanium—A review: Ore Geology Reviews, v. 30, nos. 3–4, p. 145–180. [Also available at http://dx.doi.org/10.1016/j.oregeorev.2005.07.034.]

Hu, R.-Z., Qi, H.-W., Zhou, M.-F., Su, W.-C., Bi, X.-W., Peng, J.-T., and Zhong, Hong, 2009, Geological and geochemical constraints on the origin of the giant Lincang coal seam-hosted germanium deposit, Yunnan, SW China—A review: Ore Geology Reviews, v. 36, nos. 1–3, p. 221–234. [Also available at http://dx.doi.org/10.1016/j.oregeorev.2009.02.007.]

Ishihara, Shunso, Murakami, Hiroyasu, and Marquez-Zavalia, M.F., 2011, Inferred indium resources of the Bolivian tin-polymetallic deposits: Resource Geology, v. 61, no. 1, p. 174–191. [Also available at http://dx.doi.org/10.1111/j.1751-3928.2011.00157.x.)

Jennings, Scott, and King, A.R., 2002, Geology, exploration history and future discoveries in the Red Dog district, western Brooks Range, Alaska, *in* Cooke, D.R., and Pongratz, June, eds., Giant ore deposits—Characteristics, genesis and exploration: Hobart, Tasmania, Australia, University of Tasmania, National Key Centre, Centre for Ore Deposit Research Special Publication, v. 4, p. 151–158.

Johnson, C.A., Dumoulin, J.A., Burruss, R.A., and Slack, J.F., 2015, Depositional conditions for the Kuna Formation, Red Dog Zn-Pb-Ag-barite district, Alaska, inferred from isotopic and chemical proxies: Economic Geology, v. 110, p. 1143–1156. [Also available at https://pubs.geoscienceworld.org/economicgeology/issue/110/5/.]

Jorgenson, J.D., and George, M.W., 2004, Mineral commodity profile—Indium: U.S. Geological Survey Open-File Report 2004–1300, 20 p., accessed November 30, 2015, at http://pubs.er.usgs.gov/publication/ofr20041300.

Kabata-Pendias, Alina, and Mukherjee, A.B., 2007, Trace elements from soil to human: Berlin, Germany, Springer,-Verlag, 550 p.

Kabata-Pendias, Alina, and Pendias, Henryk, 2001, Trace elements in soils and plants (3d ed.): Boca Raton, Fla., CRC Press, 413 p.

Kampunzu, A.B., Cailteux, J.L.H., Kamona, A.F., Intiomale, M.M., and Melcher, F., 2009, Sediment-hosted Zn-Pb-Cu deposits in the Central African Copperbelt: Ore Geology Reviews, v. 35, nos. 3–4, p. 263–297. [Also available at http://dx.doi.org/10.1016/j.oregeorev.2009.02.003.]

Kaneshiro, Jess, Gaillard, Nicolas, Rocheleau, Richard, and Miller, Eric, 2010, Advances in copper-chalcopyrite thin films for solar energy conversion: Solar Energy Materials and Solar Cells, v. 94, no. 1, p. 12–16. [Also available at http://dx.doi.org/10.1016/j.solmat.2009.03.032.]

Kelley, K.D., and Jennings, Scott, 2004, A special issue devoted to barite and Zn-Pb-Ag deposits in the Red Dog district, western Brooks Range, northern Alaska: Economic Geology, v. 99, p. 1267–1280. [Also available at http://dx.doi.org/10.2113/gsecongeo.99.7.1267.]

Kelley, K.D., Leach, D.L., Johnson, C.A., Clark, J.L., Fayek, M., Slack, J.F., Anderson, V.M., Ayuso, R.A., and Ridley, W.I., 2004, Textural, compositional, and sulfur isotope variations of sulfide minerals in the Red Dog Zn-Pb-Ag deposits, Brooks Range, Alaska—Implications for ore formation: Economic Geology, v. 99, p. 1509–1532. [Also available at http://dx.doi.org/10.2113/gsecongeo.99.7.1509.]

Kelley, K.D., Seal, R.R., II, Schmidt, J.M., Hoover, D.B., and Klein, D.P., 1995, Sedimentary exhalative Zn-Pb-Ag deposits (Model 31a; Briskey, 1986), chap. 29 *of* du Bray, E.A., ed., Preliminary compilation of descriptive geoenvironmental mineral deposit models: U.S. Geological Survey Open-File Report 95–831, p. 225–233, accessed November 30, 2015, at http://pubs.usgs.gov/of/1995/ofr-95-0831/CHAP29.pdf.

Krupp, R.E., and Seward, T.M., 1987, The Rotokawa geothermal system, New Zealand—An active epithermal gold-depositing environment: Economic Geology, v. 82, p. 1109–1129. [Also available at http://dx.doi.org/10.2113/gsecongeo.82.5.1109.]

Leach, D.L., Bradley, D.C., Huston, David, Pisarevsky, S.A., Taylor, R.D., and Gardoll, S.J., 2010, Sediment-hosted lead-zinc deposits in earth history: Economic Geology, v. 105, p. 593–625. [Also available at http://dx.doi.org/10.2113/gsecongeo.105.3.593.]

Leach, D.L., Sangster, D.F., Kelley, K.D., Large, R.R., Garven, Grant, Allen, C.R., Gutzmer, Jens, and Walters, Steve, 2005, Sediment-hosted lead-zinc deposits—A global perspective, *in* Hedenquist, J.W., Thompson, J.F.H., Goldfarb, R.J. and Richards J.P., eds., Economic Geology—One hundredth anniversary volume, 1905–2005: Littleton, Colo., Society of Economic Geologists, p. 561–607. [Appendixes are on a CD–ROM inside the back cover.]

Leach, D.L., Viets, J.B., Foley-Ayuso, Nora, and Klein, D.P., 1995, Mississippi Valley-type Pb-Zn deposits (Models 32a, b; Briskey, 1986a, b), chap. 30 *of* du Bray, E.A., ed., Preliminary compilation of descriptive geoenvironmental mineral deposit models: U.S. Geological Survey Open-File Report 95–831, p. 234–243, accessed November 30, 2015, at http://pubs.usgs.gov/of/1995/ofr-95-0831/CHAP30.pdf.

Lottermoser, B.G., 2010, Mine wastes—Characterization, treatment, and environmental impacts (3d ed.): Berlin, Germany, Springer-Verlag, 400 p. [Also available at http://dx.doi.org/10.1007/978-3-642-12419-8.]

Ludington, Steve, Haxel, G.B., Castor, S.B., McLaurin, B.T., and Flynn, K.S., 2006, Mineral resource potential of the Gold Butte A, Gold Butte B, Virgin Mountain (Gold Butte C), Whitney Pocket, Red Rock Spring, Devil's Throat, and Gold Butte Townsite areas of critical environmental concern, Clark County, Nevada, chap. C *of* Ludington, Steve, ed., Mineral resource assessment of selected areas in Clark and Nye Counties, Nevada: U.S. Geological Survey Scientific Investigations Report 2006–5197, p. C1–C55. [Also available at http://pubs.usgs.gov/sir/2006/5197/sir2006-5197c.pdf.]

Madden, E.F., Anderson, C.J., and Goering, P.L., 2004, Indium, chap. 12 *of* Merian, Ernest, Anke, Manfred, Ihnat, Milan, and Stoeppler, Markus, eds., Elements and their compounds in the environment—Occurrence, analysis and biological relevance: Weinheim, Germany, Wiley-VCH Verlag GmbH, pt. 3, p. 801–809. [Also available at http://dx.doi.org/10.1002/9783527619634.ch33.]

Miles, R.W., Zoppi, Guillaume, and Forbes, Ian, 2007, Inorganic photovoltaic cells: Materials Today, v. 10, no. 11, p. 20–27. [Also available at http://dx.doi.org/10.1016/s1369-7021(07)70275-4.]

Misra, K.C., Gratz, J.F., and Lu, Changsheng, 1996, Carbonate-hosted Mississippi Valley-type mineralization in the Elmwood-Gordonsville deposits, Central Tennessee zinc district—A synthesis, *in* Sangster, D.F., ed., Carbonate-hosted lead-zinc deposits—[Society of Economic Geologists] 75th anniversary volume: Littleton, Colo: Society of Economic Geologists Special Publication no. 4, p. 58–73.

Miyazaki, A., Kimura, A., and Tao, H., 2012, Distribution of indium, thallium, and bismuth in the environmental water of Japan: Bulletin of Environmental Contamination and Toxicology, v. 89, no. 6, p. 1211–1215. [Also available at http://dx.doi.org/10.1007/s00128-012-0851-0.]

Mortlock, R.A., and Froelich, P.N., 1987, Continental weathering of germanium—Ge/Si in the global river discharge: Geochimica et Cosmochimica Acta, no. 8, v. 51, p. 2075–2082. [Also available at http://dx.doi.org/10.1016/0016-7037(87)90257-2.]

Murakami, Hiroyasu, and Ishihara, Shunso, 2013, Trace elements of indium-bearing sphalerite from tin-polymetallic deposits in Bolivia, China and Japan—A femto-second LA–ICPMS study: Ore Geology Reviews, v. 53, p. 223–243. [Also available at http://dx.doi.org/10.1016/j.oregeorev.2013.01.010.]

Nagajyoti, P.C., Lee, K.D., and Sreekanth, T.V.M., 2010, Heavy metals, occurrence and toxicity for plants—A review: Environmental Chemistry Letters, v. 8, no. 3, p. 199–216. [Also available at http://dx.doi.org/10.1007/s10311-010-0297-8.]

Newlands, J.A.R., 1864, On relations among the equivalents: Chemical News, v. 10, August, p. 94–95. [Also available at http://web.lemoyne.edu/giunta/newlands.html.]

Nilsson, John, Major, Ken, Durston, Keith, Tietz, P.G., Ristorcelli, Steven, and Staargaard, C.F., 2010, Preliminary economic assessment of the Crypto zinc-copper-indium project, Juab County, Utah: Vancouver, British Columbia, Canada, Lithic Resources Ltd., 148 p. plus 5 appendixes, accessed November 30, 2015, at http://www.inzincmining.com/_resources/Lithic_Resources_Crypto_PEA_Report-opt.pdf.

Nozaki, Yoshiyuki, Lerche, Dorte, Alibo, D.S., and Snidvongs, Anond, 2000, The estuarine geochemistry of rare earth elements and indium in the Chao Phraya River, Thailand: Geochimica et Cosmochimica Acta, v. 64, no. 23, p. 3983–3994. [Also available at http://dx.doi.org/10.1016/s0016-7037(00)00473-7.]

Nozaki, Yoshiyuki, Lerche, Dorte, Alibo, D.S., and Tsutsumi, Makoto, 2000, Dissolved indium and rare earth elements in three Japanese rivers and Tokyo Bay—Evidence for anthropogenic Gd and In: Geochimica et Cosmochimica Acta, v. 64, no. 23, p. 3975–3982. [Also available at http://dx.doi.org/10.1016/s0016-7037(00)00472-5.]

Nriagu, J.O., and Pacyna, J.M., 1988, Quantitative assessment of worldwide contamination of air, water and soils by trace-metals: Nature, v. 333, no. 6169, p. 134–139. [Also available at http://dx.doi.org/10.1038/333134a0.]

Nyrstar N.V., 2013, Strategy into action—Annual report 2012: Zurich, Switzerland, Nyrstar N.V., 205 p., accessed March 1, 2016, at http://www.nyrstar.com/investors/en/Pages/reportspresentations.aspx?ff1n=Year&ff1v=2012.

Nyrstar N.V., 2016, Nyrstar Tennessee mines: Zurich, Switzerland, Nyrstar N.V., February, 2 p., accessed March 1, 2016, at http://www.nyrstar.com/operations/Documents/Fact%20Sheet%20TENNESSEE%20EN.pdf.

Obata, Hajime, Alibo, D.S., and Nozaki, Yoshiyuki, 2007, Dissolved aluminum, indium, and cerium in the Sea of Japan and the Sea of Okhotsk—Comparison to the marginal seas of the western North Pacific: Journal of Geophysical Research—Oceans, v. 112, no. C2, 10 p. [Also available at http://dx.doi.org/10.1029/2006jc003944.]

Occupational Safety and Health Administration, 2013a, Chemical sampling information—Germanium tetrahydride, CAS no. 7782–65–2: U.S. Department of Labor, Occupational Safety and Health Administration Web page, accessed November 30, 2015, at http://www.osha.gov/dts/chemicalsampling/data/CH_243200.html.

Occupational Safety and Health Administration, 2013b, Chemical sampling information—Indium and compounds (as In), CAS no. 7440–74–6: U.S. Department of Labor, Occupational Safety and Health Administration Web page, accessed November 30, 2015, at http://www.osha.gov/dts/chemicalsampling/data/CH_247101.html.

Plumlee, G.S., and Logsdon, M.J., 1999, An Earth-system science toolkit for environmentally friendly mineral resource development, *in* Plumlee, G.S., and Logsdon, M.J., eds., The environmental geochemistry of mineral deposits—Part A, Processes, techniques, and health issues: Littleton, Colo., Society of Economic Geologists, Reviews in Economic Geology Series, v. 6A, p. 1–27. [Also available at http://ebooks.geoscienceworld.org/content/the-environmental-geochemistry-of-mineral-deposits.]

Plumlee, G.S., Smith, K.S., Montour, M.R., Ficklin, W.H., and Mosier, E.L., 1999, Geologic controls on the composition of natural waters and mine waters draining diverse mineral-deposit types, *in* Plumlee, G.S., and Filipek, L.H., eds., The environmental geochemistry of mineral deposits—Case studies and research topics: Littleton, Colo., Society of Economic Geologists, Reviews in Economic Geology Series, v. 6B, p. 373–432. [Also available at http://ebooks.geoscienceworld.org/content/the-environmental-geochemistry-of-mineral-deposits.]

Ragaini, R.C., Ralston, H.R., and Roberts, N., 1977, Environmental trace metal contamination in Kellogg, Idaho, near a lead smelting complex: Environmental Science and Technology, v. 11, no. 8, p. 773–781. [Also available at http://dx.doi.org/10.1021/es60131a004.]

Reck, B.K., and Graedel, T.E., 2012, Challenges in metal recycling: Science, v. 337, no. 6095, p. 690–695. [Also available at http://dx.doi.org/10.1126/science.1217501.]

Reich, Ferdinand, and Richter, H.T., 1863, Vorläufige notiz über ein neues metall: Journal für Praktische Chemie, v. 89, no. 1, p. 441–448. [Also available at http://dx.doi.org/10.1002/prac.18630890156.]

Rockett, A.A., 2010, Current status and opportunities in chalcopyrite solar cells: Current Opinion in Solid State and Materials Science, v. 14, no. 6, p. 143–148. [Also available at http://dx.doi.org/10.1016/j.cossms.2010.08.001.]

Santosa, S.J., Wada, Satoshi, Mokudai, Hiroshige, and Tanaka, Shigeru, 1997, The contrasting behaviour of arsenic and germanium species in seawater: Applied Organometallic Chemistry, v. 11, no. 5, p. 403–414. [Also available at http://dx.doi.org/10.1002/(sici)1099-0739(199705)11:5%3C403::aid-aoc596%3E3.3.co;2-w.]

Schneider, Jens, Melcher, Frank, and Brauns, Michael, 2007, Concordant ages for the giant Kipushi base metal deposit (DR Congo) from direct Rb–Sr and Re–Os dating of sulfides: Mineralium Deposita, v. 42, no. 7, p. 791–797. [Also available at http://dx.doi.org/10.1007/s00126-007-0158-y.]

Schwarz-Schampera, Ulrich, and Herzig, P.M., 1999, Indium geology, mineralogy, and economics—A review: Hannover, Germany, Berichte zur Lagerstätten- und Rohstofforschung, Bundesanstalt für Geowissenschaften und Rohstoffe, 182 p.

Schwarz-Schampera, Ulrich, and Herzig, P.M., 2002, Indium—Geology, mineralogy, and economics: Berlin, Germany, Springer, 257 p.

Schwarz-Schampera, Ulrich, Terblanche, Hennie, and Oberthür, Thomas, 2010, Volcanic-hosted massive sulfide deposits in the Murchison greenstone belt, South Africa: Mineralium Deposita, v. 45, no. 2, p. 113–145. [Also available at http://dx.doi.org/10.1007/s00126-009-0266-y.]

Seward, T.M., Henderson, C.M.B., and Charnock, J.M., 2000, Indium (III) chloride complexing and solvation in hydrothermal solutions to 350°C—An EXAFS study: Chemical Geology, v. 167, nos. 1–2, p. 117–127. [Also available at http://dx.doi.org/10.1016/s0009-2541(99)00204-1.]

Shacklette, H.T., and Boerngen, J.G., 1984, Element concentrations in soils and other surficial materials of the conterminous United States: U.S. Geological Survey Professional Paper 1270, 105 p., accessed November 30, 2015, at http://pubs.er.usgs.gov/publication/pp1270.

Shanks, W.C. Pat, III, and Thurston, Roland, eds., 2012, Volcanogenic massive sulfide occurrence model , chap. C *of* Mineral deposit models for resource assessment: U.S. Geological Survey Scientific Investigations Report 2010–5070–C, 345 p. [Also available at http://pubs.usgs.gov/sir/2010/5070/c/.]

Shimizu, Toru, and Morishita, Yuichi, 2012, Petrography, chemistry, and near-infrared microthermometry of indium-bearing sphalerite from the Toyoha polymetallic deposit, Japan: Economic Geology, v. 107, p. 723–735. [Also available at http://dx.doi.org/10.2113/econgeo.107.4.723.]

Siebert, Christopher, Ross, Andy, and McManus, James, 2006, Germanium isotope measurements of high-temperature geothermal fluids using double-spike hydride generation MC-ICP-MS: Geochimica et Cosmochimica Acta, v. 70, no. 15, p. 3986–3995. [Also available at http://dx.doi.org/10.1016/j.gca.2006.06.007.]

Slack, J.F., Kelley, K.D., Anderson, V.M., Clark, J.L., and Ayuso, R.A., 2004, Multistage hydrothermal silicification and Fe-Tl-As-Sb-Ge-REE enrichment in the Red Dog Zn-Pb-Ag district, northern Alaska—Geochemistry, origin, and exploration applications: Economic Geology, v. 99, p. 1481–1508. [Also available at http://dx.doi.org/10.2113/gsecongeo.99.7.1481.]

Smith, D.B., Cannon, W.F., Woodruff, L.G., Garrett, R.G., Klassen, Rodney, Kilburn, J.E., Horton, J.D., King, H.D., Goldhaber, M.B., and Morrison, J.M., 2005, Major- and trace-element concentrations in soils from two continental-scale transects of the United States and Canada: U.S. Geological Survey Open-File Report 2005–1253, 20 p., accessed November 30, 2015, at http://pubs.er.usgs.gov/publication/ofr20051253.

Smith, K.S., and Huyck, L.O., 1999, An overview of the abundance, relative mobility, bioavailability, and human toxicity of metals, *in* Plumlee, G.S. and Logsdon, M.J., eds., The environmental geochemistry of mineral deposits—Part A, Processes, techniques and health issues: Littleton, Colo., Society of Economic Geologists, v. 1, p. 29–70.

SRK Consulting (Canada) Inc., 2007, Red Dog Mine closure and reclamation plan—SD B3—Plan of operations for tailings and water management —Report prepared for Teck Cominco Alaska, Inc.: Vancouver, British Columbia, Canada, SRK Consulting (Canada) Inc., SRK Project Number 1CT006.003, 8 p. [Also available at http://dnr.alaska.gov/mlw/mining/largemine/reddog/publicnotice/pdf/sdb3.pdf.]

Tanaka, Akiyo, 2004, Toxicity of indium arsenide, gallium arsenide, and aluminium gallium arsenide: Toxicology and Applied Pharmacology, v. 198, no. 3, p. 405–411. [Also available at http://dx.doi.org/10.1016/j.taap.2003.10.019.]

Tanaka, Akiyo, Hirata, Miyuki, Kiyohara, Yutaka, Nakano, Makiko, Omae, Kazuyuki, Shiratani, Masaharu, and Koga, Kazunori, 2010, Review of pulmonary toxicity of indium compounds to animals and humans: Thin Solid Films, v. 518, no. 11, p. 2934–2936. [Also available at http://dx.doi.org/10.1016/j.tsf.2009.10.123.]

Taylor, C.D., Zierenberg, R.A., Goldfarb, R.J., Kilburn, J.E., Seal, R.R., II, and Kleinkopf, M.D., 1995, Volcanic-associated massive sulfide deposits (Models 24a–b, 28a; Singer, 1986a, b; Cox, 1986), chap. 16 *of* du Bray, E.A., ed., Preliminary compilation of descriptive geoenvironmental mineral deposit models: U.S. Geological Survey Open-File Report 95–831, p. 137–144. [Also available at http://pubs.usgs.gov/of/1995/ofr-95-0831/.]

Taylor, S.R., and McLennan, S.M., 1995, The geochemical evolution of the continental crust: Reviews of Geophysics, v. 33, no. 2, p. 241–265. [Also available at http://dx.doi.org/10.1029/95RG00262.]

Tolcin, A.C., 2013a, Indium: U.S. Geological Survey Mineral Commodity Summaries 2013, p. 74–75, accessed November 30, 2015, at http://minerals.usgs.gov/minerals/pubs/commodity/indium/mcs-2013-indiu.pdf.

Tolcin, A.C., 2013b, Indium (In), *in* Metal prices in the United States through 2010: U.S. Geological Survey Scientific Investigations Report 2012–5188, p. 66–68, accessed May 24, 2016, at http://pubs.usgs.gov/sir/2012/5188/.

Tolcin, A.C., 2014, Indium: U.S. Geological Survey Mineral Commodity Summaries 2014, p. 74–75, accessed September 12, 2016, at http://minerals.usgs.gov/minerals/pubs/commodity/indium/mcs-2014-indiu.pdf.

U.S. Environmental Protection Agency, 2006, Assessment of the potential costs, benefits and other impacts of chat use in transportation projects: Washington, D.C., U.S. Environmental Protection Agency Office of Solid Waste, Reference no. S.2006.1, 81 p.

U.S. Environmental Protection Agency, 2010, Record of Decision by the U.S. Environmental Protection Agency Region 10 for the Red Dog Mine Extension Aqqaluk Project: Washington, D.C., U.S. Environmental Protection Agency, 15 p. [Also available at http://www.epa.gov/region10/pdf/permits/npdes/ak/red-dog-aqqaluk-rod.pdf.]

U.S. Environmental Protection Agency, 2013a, National primary drinking water regulations: U.S. Environmental Protection Agency, EPA 816–F–09–004, May, 6 p. [Updated version available at http://water.epa.gov/drink/contaminants/index.cfm.

U.S. Environmental Protection Agency, 2013b, NAAQS [National ambient air quality standards] table: U.S. Environmental Protection Agency Web page, accessed April 7, 2016, at https://www.epa.gov/criteria-air-pollutants/naaqs-table.

Viers, Jérôme, Dupré, Bernard, and Gaillardet, Jérôme, 2009, Chemical composition of suspended sediments in world rivers—New insights from a new database: Science of the Total Environment, v. 407, no. 2, p. 853–868. [Also available at http://dx.doi.org/10.1016/j.scitotenv.2008.09.053.]

Weeks, M.E., 1932, The discovery of the elements. XV. Some elements predicted by Mendeleeff: The Journal of Chemical Education, v. 9, no. 9, p. 1605–1619. [Also available at http://dx.doi.org/10.1021/ed009p1605.]

Weeks, R.A., 1973, Gallium, germanium, and indium, *in* Brobst, D.A., and Pratt, W.P., eds., United States mineral resources: U.S. Geological Survey Professional Paper 820, p. 237–246, accessed November 30, 2015, at http://pubs.er.usgs.gov/publication/pp820.

Wilkinson, J.J., Eyre, S.L., and Boyce, A.J., 2005, Ore-forming processes in Irish-type carbonate-hosted Zn-Pb deposits—Evidence from mineralogy, chemistry, and isotopic composition of sulfides at the Lisheen Mine: Economic Geology, v. 100, p. 63–86. [Also available at http://dx.doi.org/10.2113/100.1.0063.]

Winkler, Clemens, 1886, Germanium, Ge, ein neues, nichtmetallisches element: Berichte der deutschen chemischen Gesellschaft, v. 19, no. 1, p. 210–211. [Also available at http://dx.doi.org/10.1002/cber.18860190156.]

Wood, S.A., and Samson, I.M., 2006, The aqueous geochemistry of gallium, germanium, indium and scandium: Ore Geology Reviews, v. 28, no. 1, p. 57–102. [Also available at http://dx.doi.org/10.1016/j.oregeorev.2003.06.002.]

Xuexin, Song, 1984, Minor elements and ore genesis of the Fankou lead-zinc deposit, China: Mineralium Deposita, v. 19, no. 2, p. 95–104. [Also available at http://dx.doi.org/10.1007/bf00204667.]

Ye, Lin, Cook, N.J., Ciobanu, C.L., Yuping, Liu, Qian, Zhang, Tiegeng, Liu, Wei, Gao, Yulong, Yang, and Danyushevskiy, Leonid, 2011, Trace and minor elements in sphalerite from base metal deposits in South China—A LA-ICPMS study: Ore Geology Reviews, v. 39, no. 4, p. 188–217. [Also available at http://dx.doi.org/10.1016/j.oregeorev.2011.03.001.]

Young, L.E., 2004, A geologic framework for mineralization in the western Brooks Range, Alaska: Economic Geology, v. 99, p. 1281–1306.

Zeh, Armin, Jaguin, Justine, Poujol, Marc, Boulvais, Philippe, Block, Sylvain, and Paquette, J.-L., 2013, Juvenile crust formation in the northeastern Kaapvaal Craton at 2.97 Ga—Implications for Archean terrane accretion, and the source of the Pietersburg gold: Precambrian Research, v. 233, p. 20–43. [Also available at http://dx.doi.org/10.1016/j.precamres.2013.04.013.]

Zurita, J.L., Jos, Angeles, del Peso, Ana, Salguero, Manuel, Cameán, A.M., López-Artíguez, Miguel, and Repetto, Guillermo, 2007, Toxicological assessment of indium nitrate on aquatic organisms and investigation of the effects on the PLHC-1 fish cell line: Science of the Total Environment, v. 387, nos. 1–3, p. 155–165. [Also available at http://dx.doi.org/10.1016/j.scitotenv.2007.07.057.]

For more information concerning this report, please contact:
Mineral Resources Program Coordinator
U.S. Geological Survey
913 National Center
Reston, VA 20192
Telephone: 703–648–6100
Fax: 703–648–6057
Email: minerals@usgs.gov
Home page: https://minerals.usgs.gov

Prepared by the USGS Science Publishing Network
Reston Publishing Service Center
Edited by J.C. Ishee and Stokely J. Klasovsky
Illustrations by Caryl J. Wipperfurth
Layout by Caryl J. Wipperfurth and Cathy Y. Knutson
Posting by Angela E. Hall

ISSN 2330-7102 (online)
https://doi.org/10.3133/pp1802I